

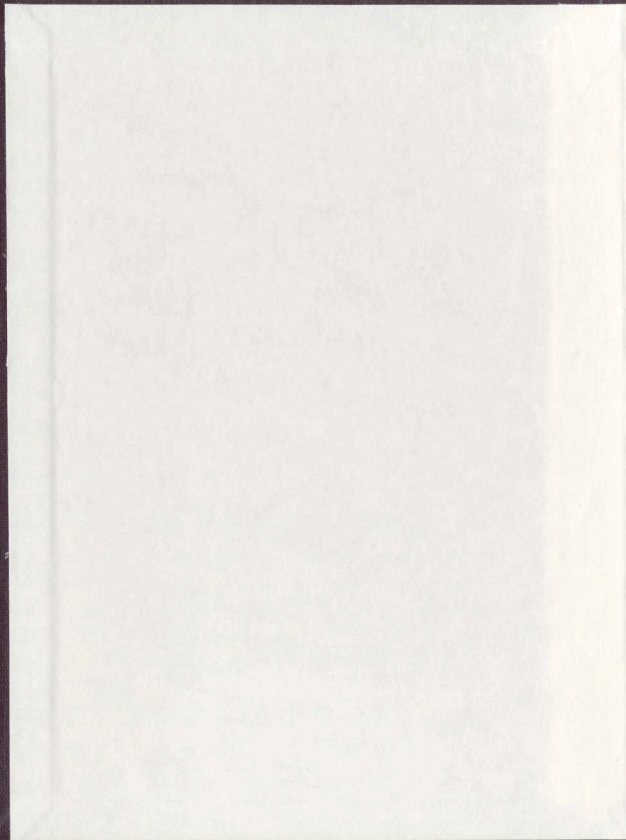
PHYSICAL AND CHEMICAL CHARACTERIZATION AND
UPGRADING OF CHAR DERIVED FROM SCRAP TIRES
BY ULTRA FAST PYROLYSIS

CENTRE FOR NEWFOUNDLAND STUDIES

**TOTAL OF 10 PAGES ONLY
MAY BE XEROXED**

(Without Author's Permission)

NEVENA POPOVIC



INFORMATION TO USERS

This manuscript has been reproduced from the microfilm master. UMI films the text directly from the original or copy submitted. Thus, some thesis and dissertation copies are in typewriter face, while others may be from any type of computer printer.

The quality of this reproduction is dependent upon the quality of the copy submitted. Broken or indistinct print, colored or poor quality illustrations and photographs, print bleedthrough, substandard margins, and improper alignment can adversely affect reproduction.

In the unlikely event that the author did not send UMI a complete manuscript and there are missing pages, these will be noted. Also, if unauthorized copyright material had to be removed, a note will indicate the deletion.

Oversize materials (e.g., maps, drawings, charts) are reproduced by sectioning the original, beginning at the upper left-hand corner and continuing from left to right in equal sections with small overlaps.

Photographs included in the original manuscript have been reproduced xerographically in this copy. Higher quality 6" x 9" black and white photographic prints are available for any photographs or illustrations appearing in this copy for an additional charge. Contact UMI directly to order.

Bell & Howell Information and Learning
300 North Zeeb Road, Ann Arbor, MI 48106-1346 USA
800-521-0600

UMI[®]



National Library
of Canada

Acquisitions and
Bibliographic Services

395 Wellington Street
Ottawa ON K1A 0N4
Canada

Bibliothèque nationale
du Canada

Acquisitions et
services bibliographiques

395, rue Wellington
Ottawa ON K1A 0N4
Canada

Your file / Votre référence

Our file / Notre référence

The author has granted a non-exclusive licence allowing the National Library of Canada to reproduce, loan, distribute or sell copies of this thesis in microform, paper or electronic formats.

The author retains ownership of the copyright in this thesis. Neither the thesis nor substantial extracts from it may be printed or otherwise reproduced without the author's permission.

L'auteur a accordé une licence non exclusive permettant à la Bibliothèque nationale du Canada de reproduire, prêter, distribuer ou vendre des copies de cette thèse sous la forme de microfiche/film, de reproduction sur papier ou sur format électronique.

L'auteur conserve la propriété du droit d'auteur qui protège cette thèse. Ni la thèse ni des extraits substantiels de celle-ci ne doivent être imprimés ou autrement reproduits sans son autorisation.

0-612-54949-6

Canada

**Physical and Chemical Characterization and Upgrading of Char
Derived from Scrap Tires by Ultra Fast Pyrolysis**

by

Nevena Popovic

A thesis submitted to the School of Graduate Studies in partial fulfilment of
requirements for the degree of Master of Science

Memorial University of Newfoundland
St. John's, Newfoundland, Canada

February 2000

ABSTRACT

In the search for a commercially efficient technology for solving the problem of scrap tires, pyrolysis is accepted as an environmentally and economically attractive recycling method to recover useful products from scrap tire waste. Ireton International Waste Management is commercially developing an ultra fast pyrolysis technology called the Continuous Ablative Reactor (CAR) which can heat solid particles to a high temperature (500-600 °C) in under one second. The pyrolytic char obtained in this ultra fast pyrolysis process has been characterized and efforts were made to upgrade the product. EnerVision Inc. (Halifax) provided samples from their pilot unit. Initial investigations were focused on the char in its original form. The char contained inorganic compounds present in tires, along with the original carbon black and a substantial amount of condensed organic by-products formed during the pyrolysis process. The contaminants in the char were reflected in an oily appearance, specific odour and high ash content. These contaminants can be eliminated, or significantly reduced. The economic feasibility of the process depends on the char quality and its usefulness in high value commercial applications.

High temperature heat treatments (600-900 °C) and oxidation processes using various agents (i.e., air, H₂O₂, HNO₃) present an opportunity to elevate the char quality and improve its commercial value. In this study, it was demonstrated that the production of highly activated char is possible by activation using steam or carbon dioxide. The adsorption

properties of the activated char so obtained were found to be comparable to those of the commercial active carbons. Hence, ultra fast pyrolysis may provide a recycling alternative for waste tires and for the production of new adsorbents from low-cost waste material.

Analytical techniques used in characterizing the chars and activated chars (and described in this thesis) included flame atomic absorption, scanning electron microscopy, transmission electron microscopy, Malvern particle size counting, Raman spectroscopy, FT-infrared spectroscopy, N₂ and CO₂ adsorption studies, and sequential pyrolysis GC-MS.

ACKNOWLEDGMENTS

I would like to take this opportunity to thank my supervisor Dr. Robert Helleur for his continued support and guidance throughout the study.

I am thankful to Dr. Christopher Flinn and Dr. Chris Parrish, members of my supervisory committee, for valuable advice.

My gratitude is expressed to Dr. Michio Ikura, Dr. Liu Dirkson, Ron Campbell and Dr. Maria Stanculescu from CANMET, Energy Technology Centre, Natural Resources Canada for valuable cooperation on the project.

I wish to express my appreciation to Mrs. Linda Thompson and Mr. Milorad Popovic for their support and encouragement.

Financial support from N.S.E.R.C., The Department of Chemistry and The School of Graduate Studies, Memorial University, are gratefully acknowledged.

GLOSSARY

AAS	Atomic Absorption Spectroscopy
BET	Brunauer, Emmett and Teller Equation (Surface Area by Gas Adsorption)
CAR	Continuous Ablative Reactor
DFT	Density Functional Theory
FTIR	Fourier-Transform Infrared Spectroscopy
GC	Gas Chromatography
Py-GC-MS	Pyrolysis-Gas Chromatography-Mass Spectrometry
SEM	Scanning Electron Microscopy
TEM	Transmission Electron Microscopy
TGA	Thermogravimetric Analysis
TPD	Temperature Programmed Desorption
XRF	X-Ray Fluorescence

TABLE OF CONTENTS

ABSTRACT	i
ACKNOWLEDGMENTS	iii
GLOSSARY	iv
LIST OF FIGURES	ix
LIST OF TABLES	xi
CHAPTER 1: INTRODUCTION	1
1.1 Scrap Tires and Their Recycling	1
1.2 Objectives	4
1.3 Literature Review on Char	5
1.4 Ultra Fast Pyrolysis of Scrap Tires	8
1.5 Carbon Black	11
1.6 Carbon Black Characterization	12
1.7 Active Carbon	14
CHAPTER 2: EXPERIMENTAL	20
2.1 Bulk Analysis Methods	20
2.1.1 Elemental Analysis	20
2.1.2 Heating Loss	21

2.1.3	Ash	21
2.1.4	X-Ray Fluorescence (XRF)	21
2.1.5	Thermogravimetric Analysis (TGA)	22
2.1.6	Atomic Absorption Spectroscopy (AAS)	22
2.1.7	Iodine Number Surface Area	23
2.1.8	Surface Area and Pore Size Distribution by Gas Adsorption	23
2.1.9	Toluene Discoloration	24
2.1.10	pH	24
2.1.11	Particle Size Measurement	25
2.1.12	Aggregate Size Measurement	25
2.1.13	Raman Spectroscopy	26
2.1.14	Infrared Spectroscopy (FTIR)	26
2.1.15	Scanning Electron Microscopy (SEM)	26
2.2	Char Demineralization	27
2.3	Heat Treatment (Carbonization)	27
2.4	Surface Group Analysis	28
2.5	Oxygenated Surface Group Analysis by Pyrolysis GS-MS	29
2.6	Adsorption Capacity	29
2.6.1	Methylene Blue Adsorption	29
2.6.2	Phenol Adsorption	30
2.6.3	Metal Ions Adsorption	30

2.7	Oxidation of Char	31
2.8	Char Activation	31
2.9	Use of Molasses as Binder	33
CHAPTER 3: RESULTS		35
3.1	Bulk Analysis of Pyrolytic Char and Commercial Carbon Black	35
3.1.1	Samples	35
3.1.2	Physico-Chemical Properties	35
3.1.3	Chemical Composition of Ash from Char	39
3.1.4	IR and Raman Spectroscopic Analysis	41
3.1.5	SEM and TEM Micrographs	44
3.1.6	Particle and Aggregate Size Distribution	44
3.2	Demineralization of Char	45
3.3	Carbonization of Char	48
3.4	Oxidation of Char	51
3.5	Activated Char	53
3.6	Use of Molasses as Binder	54
3.7	Pore Size Distribution of Activated Char	57
CHAPTER 4: DISCUSSION		58
4.1	Physico-Chemical Properties of Untreated Pyrolytic Char	58

4.2	Char Demineralization	65
4.3	Carbonization Process	66
4.3.1	Physical and Chemical Characteristics	66
4.3.2	Adsorption Capacity	70
4.4	Char Oxidation	74
4.5	Activation and Activated Char	79
4.5.1	General Characteristics	79
4.5.2	Porosity, Surface Area and Adsorption Capacity.....	82
4.6	Molasses as Binder	91
4.7	Other Activation Studies	92
CHAPTER 5: SUMMARY		96
REFERENCES		100

LIST OF FIGURES

1.1	Schematic of the CAR Pyrolysis Unit	9
2.1	Carbonization/Activation Unit	32
3.1	Raman Spectra of (a) Untreated Char, (b) Carbonized Char and (c) Carbon Black.....	43
4.1	TEM Micrographs of (a) Char C1 and (b) Commercial Carbon Black	62
4.2	Particle Size Distribution Curves for Char C1 and Commercial Carbon Black	63
4.3	Aggregate Size Distribution of Char C1	64
4.4	TEM Micrographs of Char Carbonized (a) at 600 °C and (b) at 900 °C	68
4.5	(a) Particle and (b) Aggregate Size Distribution of Carbonized Char at 900 °C	69
4.6	Correlation Between Surface Area Measured by BET and by Iodine Number	71
4.7	Classification of Surface Groups by Boehm Titration of Carbonized Char (600 °C), Oxidized by Air, by H ₂ O ₂ , by HNO ₃ and Carbon Black	75
4.8	TPD Profiles of CO (m/z: 28) and CO ₂ (m/z: 44) Production from Carbonized Char (600 °C) and Air Oxidized Char	78
4.9	Correlation Between Surface Area and Mass Loss Resulting from Char Activation	81
4.10	N ₂ Adsorption/Desorption Isotherms of Steam Activated Chars	83
4.11	DFT Pore Size and Pore Volume Distribution of Steam-Activated Chars	85

4.12	DFT Pore Size and Pore Volume Distribution of CO ₂ -Activated Char and its Precursor	86
4.13	CO ₂ Adsorption/Desorption Isotherm of Char Activated by CO ₂	87
4.14	SEM Micrographs of Char Carbonized (a) at 600 °C and (b) at 900 °C	89
4.15	SEM Micrographs of Char Activated (a) by Steam and (b) by CO ₂	90
4.16	SEM Micrographs of Char Blended with 20 % Molasses Followed by Activation Using Steam	93

LIST OF TABLES

1.1	Typical Composition of Tire Rubber	2
3.1	Physico-Chemical Properties of Commercial Carbon Black Grades Used as Reference Standards	37
3.2	Chemical Composition of Pyrolytic Char from Tire Pyrolysis by Different Investigators and of Commercial Carbon Black	38
3.3	Physico-Chemical Characteristics of the Char Samples	39
3.4	Chemical Composition of Char by XRF Analysis	40
3.5	Chemical Composition of Ash from Char by SEM	41
3.6	<i>Chemical Composition of Ash from Char by AAS</i>	41
3.7	Parameters of the Raman Peaks of Char and Commercial Carbon Black	42
3.8	Ash Content of Chars, wt. %, as a Function of Acid Concentration, Reaction Temperature and Time	46
3.9	Zn Content in Ash of Chars Treated with Different Acids and Using <i>Different Concentrations Measured by AAS</i>	47
3.10	Acid Wash Efficiency of Other Elements Measured by SEM	47
3.11	Physico-Chemical Characteristics of Char C1 Carbonized at Different Temperatures	49
3.12	Chemical Composition of Ash from Carbonized C1 by AAS	49
3.13	Titration of Acidic Groups of Carbonized Char and Commercial Carbon Black ...	50

3.14	Adsorption Capacity of Carbonized Char and Commercial Active Carbon	51
3.15	Titration of Acidic Groups of Oxidized Char	52
3.16	Iodine Number of Oxidized Char and Adsorption Capability for Methylene Blue, Phenol, Pb^{2+} and Cu^{2+}	52
3.17	Elemental Analysis of Char Carbonized at 600° C and Oxidized Char Samples	53
3.18	Char Activation Conditions	55
3.19	Surface Area and Adsorption Capacity of Activated Char and Commercial Active Carbon	56
3.20	Titration of Acidic Surface Groups of Activated Char Blended with Molasses	57
3.21	Surface Area and Adsorption Capacity of Activated Char Blended with Molasses	57

CHAPTER 1

INTRODUCTION

1.1 Scrap Tires and Their Recycling

Europe, the United States of America and Japan together generate more than 5×10^6 tonnes of scrap tires a year. According to recent statistics, the populations of the USA and Canada together dispose of over one tire per person per year. Other world communities like South East Asia have also recorded a rapid growth in automobile ownership and, as a consequence, have increased scrap tire generation. The US Environmental Protection Agency (1993) predicts a 15-20 % increase by the early 21st century [1]. Such a rapidly increasing trend and the fact that the majority of these tires are stockpiled on landfills present one of our most potentially hazardous material disposal problems of today. Tires are made up of ingredients such as styrene-butadiene rubber, carbon black, silica and other chemicals used for curatives and processing aids, as listed in Table 1.1 [2]. These are carefully selected on the basis of their physico-chemical properties and mutual interactions to provide a wide range of mechanical properties.

To reduce the negative environmental impacts such as those caused by disposal of scrap tires (a non-biodegradable waste) in landfills or by incineration, constituent chemicals

and energy content can be recovered by a number of available technologies.

Table 1.1 Typical Composition of Tire Rubber

Component	wt. %
Styrene-butadiene copolymer	62.1
Carbon black	31.0
Extender oil	1.9
Zinc oxide	1.9
Stearic acid	1.2
Sulfur	1.1
Accelerator	0.7
Total	99.9

The conventional methods for energy recovery are based on simple combustion in cement kilns or co-combustion with coal. Shredded or powdered scrap tires can be added as a filler for asphalt in road pavement (about 2.2 tonnes/km). Also, tire powder is often used as compounding for low-value rubber goods. However, all these applications combined do not solve the scrap tire stockpiling problem and does not result in adequate profitability.

Pyrolysis is an established process method, but its use in tire pyrolysis is on a laboratory scale and industrial trials are relatively new. Basically, pyrolysis involves the decomposition of organic wastes at high temperatures in an inert atmosphere or under

vacuum. This process presents an alternative to scrap tire disposal in landfill sites and can result in the recovery of useful products in an environmentally-friendly manner. The products recovered by a typical pyrolysis process are usually: 33-38 wt. % pyrolytic char, 38-55 wt. % oil and 10-30 wt. % gas fraction. Typical product yields are a function of pyrolysis conditions such as temperature and heating rate [3]. The recovered gas consists of hydrogen, carbon dioxide, carbon monoxide, methane, ethane and butadiene, with lower concentrations of propane, propene, butane and other hydrocarbon gases [3]. This gas mixture has a high calorific value $\sim 37 \text{ MJ/m}^3$ [1], sufficient to heat the pyrolysis reactor or be combusted in conventional gas burners.

The pyrolytic oil contains many valuable hydrocarbons and therefore can be used as a source of chemical feedstock such as limonene, benzene, toluene, xylene etc. Due to its high calorific value of $\sim 43 \text{ MJ/kg}$ [2], the oil can also be used as a fuel. This oil may also be used as a feed blend in refinery operations.

The carbonized particulate residue referred to as char is a carbon-rich solid material. Char originates from the reinforcing carbon black used as a filler in tire production. However, char also contains almost all the inorganic compounds present in tires and a substantial amount of the condensed by-products formed during the pyrolysis process. Consequently, its yield exceeds the actual amount of carbon black present in scrap tires. Char may be used as a solid fuel because of its combustion heat of $\sim 30 \text{ MJ/kg}$. Its ignition

temperature is approximately 510 °C [4].

Generally, the pyrolysis products do not possess properties of sufficiently high quality to be reused as raw materials owing to the complexity of the mixtures and the presence of contaminants such as ash and sulfur-containing by-products. Upgrading is a necessary step which is needed to justify the cost of the pyrolysis.

The direction of this study was determined by the origin of char, namely from the pyrolysis of rubber tires, and by the desirability of recycling carbon black-quality char to the rubber compounding industry, an industry which consumes 90 % of the 7×10^6 tonnes annual carbon black production.

1.2 Objectives

The objectives of this study were the characterization and improvement of the properties of the char produced by ultra fast pyrolysis using the Continuing Ablative Reactor (CAR) technology, specifically:

- examination of the properties of char related to the requirements of the rubber industry and comparison with commercial carbon black grades,
- reduction of inorganic impurities in char using mineral acid and base treatments,

- elimination of adsorbed hydrocarbons (oil) and pyrolytic carbon deposits using post pyrolysis heat treatments,
- investigation of the adsorption capacity of chars and oxidized chars to produce an effective adsorbent without activation,
- optimization of char activation using steam, oxygen or carbon dioxide treatment to maximize adsorption performance.

1.3 Literature Review on Char

Research on the use of scrap tires for the production of char has been undertaken in laboratory and pilot-scale units for many years. Many authors claim that the characteristics of the recovered char (or carbon black) depend on the pyrolysis operating conditions and scrap tire compositions. Beckman *et al.* [5] suggested that “pyrolysis of scrap tires in an inert atmosphere is essentially a carbon black recovery process”.

Various scrap tire pyrolysis processes, such as fluidized beds, a shaft furnace, an extruder and a rotary kiln, had been studied in Japan for a few years before an actual 7,000 t/y capacity plant with a rotary kiln process was constructed. Kawakami *et al.* [6] found a relationship between pyrolysis temperature and the quality of the produced char. To avoid increased cohesion forces between carbon particles in the char, and the consequent poor dispersion ability in rubber production, it was suggested that a temperature limit of 600 °C

in the pyrolysis process should not be exceeded. The same temperature limit was suggested for the subsequent char refining process. Truck tires produced from the recovered carbon black showed sufficient durability in laboratory and road tests. These results were comparable with those produced by commercial “general purpose furnace black - GPF” and “high abrasion furnace black - HAF”.

Crane *et al.* [7] promoted a process of scrap tire pyrolysis in a steam atmosphere. It was found that the carbon black produced had a very clean surface, without tarry deposits, and possessed characteristics of the original carbon black which was used in tire production.

Teng *et al.* [3] compared the chemical structure of the rubber tire with that of coal and carried out an oxidation pretreatment before pyrolysis. It was found that high pressure oxygen pretreatment of tires would increase the oxygen functional group content which favors cross linking reactions during pyrolysis, thereby increasing char yield. This approach may be important if char yield in a pyrolysis process is to be maximized.

Dodds *et al.* [8] reported that the pyrolytic carbonaceous material from tires contains carbon with a substantial solid hydrocarbon fraction and metal oxides. The solid hydrocarbon fraction can be avoided by increasing the pyrolysis temperature. However, the primary structure of the original carbon black seems to degrade when pyrolysis is conducted at temperatures higher than 380 °C.

The scrap tire vacuum pyrolysis process developed by Roy at Laval University, Quebec, operates under sub-atmospheric pressures ranging from 0.3 to 20 kPa and temperatures ranging from 420 to 700 °C [9]. It was shown that both pyrolysis temperature and pressure have a major influence on the properties of the recovered carbon black (char). Pyrolytic carbon deposits on carbon black decrease with lowering of pressure and increase with pyrolysis temperature.

Many authors [1 and 10] have investigated the use of pyrolytic char as a precursor for active carbon production. Torkai, Meguro and Nakamura [11] pyrolysed scrap tires at 550 °C and produced char activated by carbon dioxide at 900 °C. The activated char surface area was measured at 400 m²/g, but activation resulted in a high 80 % burn-off. A linear relationship was observed between activation time and burn-off, as well as burn-off and surface area.

Ogasawara *et al.* [12] performed pyrolysis and activation in one stage in a helium atmosphere with a continuous water injection. The active char product obtained had a very high surface area (1260 m²/g), comparable to that of commercial active carbon. However, the product yield was only 9 %. Teng *et al.* [3] concluded that the surface area of the char increased with char burn-off. Their activation process with carbon dioxide resulted in a maximum surface area of 370 m²/g with 50 % burn-off. Merchant and Petrich [4] have demonstrated the conversion of scrap tire char into active carbon with a surface area of 500

m²/g at 850 °C in an atmospheric pressure nitrogen stream containing 40 mol % water. The burn-off was 40 %.

In terms of activated char application, San Miguel *et al.* [1] showed that tire char possesses relatively high adsorption capacity for aqueous species of large molecular weight. They proposed its application in textile effluent treatment thus avoiding the use of more costly activated carbon. Lehmann *et al.* [13] evaluated tire-derived active carbon as a gas clean-up adsorbent and obtained adsorption capacity results for acetone, trichlorethane, mercury (I) and mercury (II) chloride comparable to those of commercial active carbon.

1.4 Ultra Fast Pyrolysis of Scrap Tires

To perform successful pyrolytic decomposition and maximize recovery of the primary pyrolysis products while minimizing secondary polymerization and condensation reactions, a fast pyrolysis process should be established where kinetic and operational parameters are favorable. In order to meet these requirements a number of fast reactor designs have been developed [14]. In this study the char produced by the Continuous Ablative Reactor (CAR), Figure 1.1, recently developed by International Waste Management, was analyzed. This device heats solid particles to a high temperature by ablation on a hot surface in under one second. The reactor, operating at 550 °C, provides very high heat and mass transfer ratios within short residence times (0.5-2 s) without the need for recycling of solids. The reactor

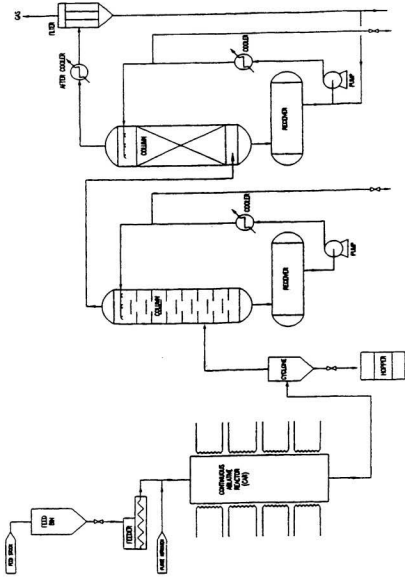


Figure 1.1 Schematic of the CAR Pyrolysis Unit

geometry and fast carrier gas flow constrain the solid against a hot metal surface thereby generating a high heat transfer rate and a high temperature. Inside the pyrolysis reactor, the rate of conversion is controlled by the heat transfer rate. The CAR design optimizes this. The same mechanism which forces the reaction material across the hot surface also peels away the hot outer surface (ablation) of treated material [14]. Thus, hot products are instantaneously removed maintaining steady-state conditions and a high mass transfer rate between phases, thereby increasing heat conductivity in particles (due to intimate contact between them). The high velocities of the particles along with product transport in the self-containing system results in a short residence time and reduced reactor volume thereby reducing the amount of associated equipment.

Shredded scrap tire material, with the steel belt removed, is conveyed to the feed bin and through a flexible chute, where it is combined with a stream of preheated purge gas and directed to the reactor. The purge gas, usually nitrogen, is used to assist in removing the vapor products from the reactor and to control the velocity (residence time) of particle flow. The products from the reactor are directed into a cyclone system where pyrolytic char is separated from the hot vapor stream. The char is discharged through to the hoppers. The hot vapor phase, a mixture of condensable and non-condensable fractions, is piped to the condensing columns in the quenching system. Liquid hydrocarbons are separated from the gaseous product. The gas leaving the separating columns passes a secondary cooler and a mist filter to upgrade the quality of gas for combustion use.

1.5 Carbon Black

Carbon black, an amorphous material composed of elemental carbon in the form of near-spherical particles fused together into aggregates, is produced by controlled partial oxidation or thermal decomposition of heavy residual oil or hydrocarbon gases. The unique ability of carbon black to enhance the physical and mechanical properties of tire elastomers by improving treadwear and traction, reducing rolling resistance and keeping heat generation at a minimum, makes it an important integral component in tire production. The rubber industry, the largest carbon black consumer, uses 90 % of total world production which exceeds 7×10^6 tonnes per year [15]. An automobile tire without carbon black reinforcement can only last about 1000 miles, while service life is extended 40-fold when carbon black is incorporated. There are two groups of carbon black properties which provide its reinforcing ability. One is related to morphology and the other to surface chemistry. Primary particle size, porosity, aggregate size and shape are important morphological properties, while surface chemistry is determined by specific surface area and the nature of the functional groups which are present [15].

In the non-rubber applications such as pigments and plastics production, carbon black fulfills a wide range of specific requirements. Important attributes of carbon black as xerographic toner are the electrical charging and flow properties of the particles [15]. Carbon black is also a semi-conductor. Its conductivity, enhanced by high structure, high porosity

and clean surface, plays an intrinsic role in its use in conductive polymer production. Such polymers are important for production of electronic, telephone and power cables.

For such a variety of demands, many grades of carbon black have been developed. For the rubber industry alone, 40 different types of carbon black are available. This study attempts to explore the end use of pyrolytic char produced from used tire by thoroughly characterizing its physical and chemical properties.

1.6 Carbon Black Characterization

Particle size: Particle size is a crucial characteristic of carbon black in all fields of its application, is primarily determined by the temperature profile in a reactor during its production. The particles are essentially geometric entities whose average dimensions range from a few to several hundred nm [15]. When carbon black particles are formed they do not exist in isolation. They are extensively fused together by covalent bonds into chains or clusters called aggregates. Aggregates are rigid colloidal entities in the nm or μm size range and are often defined as the smallest dispersible unit [15]. Due to their reactive nature, carbon surface aggregates exhibit a very strong tendency to form weak inter-aggregate bonds, thereby forming agglomerates. Aggregates are considered to be unbreakable formations while agglomerates are easily disintegrated during normal carbon black processing [15]. Primary particle size and aggregate size are characterized by their distributions. The size and bulkness

of aggregates and agglomerates define carbon black structure. Low and high structure are synonyms for carbon blacks consisting of small and large aggregates and agglomerates, respectively.

Porosity: Porosity is a fundamental morphological property of carbon black. The degree of porosity is affected by the conditions of the production process. Porosity affects surface area and increases the effective loading of carbon black [15]. There are two categories of porosity: 1) “open porosity” consisting of nm size pores on the carbon black surface; and 2) “closed porosity” in particles, or within an aggregate inaccessible to the external surface. Gas adsorption techniques and density methods reveal the extent of porosity.

Surface area: Surface area is defined as the available area on the carbon black surface and in its accessible pores. As with all solids, carbon black interacts with other substances via its surface. There is a geometrical relationship between particle size and surface area. Non-porous carbon black surface area has an inverse correlation with particle size [15]. However, particles do not exist as separate entities so aggregates have to be considered.

Specific surface area is the value of the surface area per gram of material. It may be determined by methods based on the adsorption on the surface of carbon black of specified molecules such as nitrogen, cetyl-trimethyl-ammonium-bromide (CTAB), iodine, etc.

The surface area reflects morphological properties and accidental geometry of carbon black. In addition, adsorbed surface groups with their chemical reactivity contribute to the phenomenon termed “reinforcement”, defined as improvement in the service life of a rubber article. This reinforcement is distinctive among the other fillers and provide a unique ability to enhance the physical properties of elastomers. It is believed that carbon black surface activity which originates from surface groups has an essential effect on the nature of the interaction between carbon black and the polymer matrix [16].

The surface area and structure of carbon black are used in its classification and characterization. Knowledge of the surface area and structure of carbon black enables a prediction of its dispersion (i.e., the rheology) properties and optimal fillers loading.

1.7 Active Carbon

Active carbon is a carbonaceous material with a highly developed internal surface area and with a very large adsorptive power. Adsorption potential of active carbon is related to its surface area, pore size distribution and the chemical reactivity of the surface. Active carbons are widely used in waste water treatments, for chemical recovery and decolorizing. Often, active carbon is the material of choice in the air-pollution control operations, for use in gas storage, separation and clean-up applications.

Theoretically, any carbonaceous material, natural or synthetic, can be converted into active carbon by an appropriate thermal treatment followed by a chemical or physical activation process. However, in a number of technical applications the adsorption capacity of active carbon is not the first concern. Cost becomes an important consideration when the active life of a material is low for various reasons, and regeneration is not economical. A number of technologies have been developed for active carbon production from inexpensive precursors.

Manufacture: Active carbon is produced by the carbonization of suitable carbonaceous material (nutshells, coals, woods etc.) followed by its activation. Activation can be physical or chemical. Carbonization is an actual pyrolysis conducted at 600-650 °C in an inert atmosphere. During the carbonization process hydrogen and oxygen are stripped off and the resulting free radicals condense to become a rigid cross-linked solid char [17].

Physical activation: Carbonization can be followed by physical activation, where a pore system is developed using oxidizing agents such as carbon dioxide, steam, air or even some mixture of these, heated to 700-1100 °C. Under optimal process conditions (oxidizing agent, temperature, flow rate and pressure) burn-off or oxidation of carbon atoms takes place. The process is complicated and understood only in general terms [17]. Generally, in activation at high temperature, an activating agent diffuses into the char pores causing a chemical reaction with the carbon atoms and loss of carbon. A proposed mechanism of

activation can be found in references 17 and 18.

For example, oxygen from the oxidizing agent CO_2 reacts with the less organized carbon atoms from the char producing the carbon-oxygen complex. The carbon oxygen-complex subsequently produces a molecule of carbon monoxide, thereby eliminating a carbon atom from the char particle thus creating new active sites (pores). These pores have an irregular structure. However, when the oxidizing agent attacks the carbon atoms in layers of crystallites, partial burn-off leads to the formation of pores with a more regular structure. The activation rate of char (with oxidizing agent) is influenced by factors such as char composition, ash content, internal pore surface area and by temperature and reaction time.

Chemical activation: Chemical activation is also a common method for active carbon production. In chemical activation, the first step is impregnation of the parent material with reagents such as zinc chloride, phosphoric acid, potassium sulphide or potassium carbonate. In the second step, the precursor and chemical activant are carbonized together at temperatures between 600 to 850 °C. If phosphoric acid is used, the temperature is much lower, i.e., 400 °C. After carbonization/activation the chemical agent is recovered by leaching and the active carbon is dried. There are however, environmental concerns with the use of the activation agents, because they are considered hazardous chemicals in the pollution regulations. In addition, chemical activation poses problems such as lack of adequate control over porosity development [17].

Porosity and surface area: During the activation process disorganized carbon atoms are removed from the spaces between the elementary crystallites of carbon particles. Organized carbon atoms from the graphitic layers of these crystallites may also be removed, thereby creating a larger number of pores. The total surface area of the pore walls (internal surface) in active carbon is very large in comparison with area of its outer surface. Therefore, this is the main reason for its large adsorption capacity [18]. The extent of pore development depends on the nature of the starting material, the composition of the activation atmosphere, the temperature and the duration of the activation process. Pores are classified into three main groups:

- a) micropores, width less than 2 nm
- b) mesopores, width between 2 and 50 nm
- c) macropores, width above 50 nm

Each of these three pore types has its specific function in the adsorption process [18]. However, due to its large surface area (often above 1000 m²/g) microporous material is of the greatest significance for active carbon adsorption capacity. The difference in pore size distribution affects the adsorption capacity for adsorbate molecules of different sizes and shapes, and this distribution is one of the criteria by which carbons are selected for any particular application. Micropores contribute mostly to high surface areas of active carbon and provide high adsorptive capacities for molecules of small dimensions such as gases or

common solvents. Mesopores are important for the adsorptions of bigger molecules such as colorants. Macropores are not very important for the adsorption processes and their role is to serve as feeder pores for the transport of adsorbate molecules.

The surface area of porous solids cannot be measured in absolute terms. The simple reason is that there does not exist an appropriate or standard method for a reliable surface area determination. Instead, its numerical value represents an assumption of adsorbate monolayer coverage and is a function of the methodology. All that is required of a porous solid is a knowledge of how much of a given adsorbate it will adsorb under defined conditions of concentration and temperature [17]. The most preferred method is the adsorption of nitrogen at 77 K, with the resulting isotherm interpreted by the Brunauer, Emmett and Teller (BET) equation. The adsorption isotherm provides an estimate of surface area and pore volumes and an assessment of the surface chemistry.

Surface Chemistry: “Nearly every type of functional group known in organic chemistry has been suggested as being present on the surface of activated carbon”, according to James S. Mattson *et al.* [19]. These functional groups influence the physico-chemical properties of carbon such as its catalytic potential, wettability and chemical reactivity. Adsorption, as a surface phenomenon, is determined not only by carbon structure (surface and pore system) but by chemical groups containing oxygen or heteroatoms. Groups on the surface can have acidic, basic or neutral character. Acidic surface groups are formed during

carbon reaction with oxygen or other oxidizing agent at temperatures up to 400 °C. The basic groups on active carbon surface are formed by high temperature heat treatment up to 1000 °C in an inert atmosphere or in a vacuum, followed by direct reaction with oxygen at room temperature. The neutral surface groups have an ethylenic structure and they are formed by the irreversible adsorption of oxygen at unsaturated sites present on the carbon surface.

CHAPTER 2

EXPERIMENTAL

Unless otherwise noted experiments were conducted at Memorial University.

2.1 Bulk Analysis Methods

2.1.1 Elemental Analysis

Carbon, hydrogen and nitrogen were determined by a combustion method using a Perkin Elmer 240C Elemental Analyzer at CANMET. According to their procedure, a 2 mg sample was introduced into a combustion tube set at 1000 °C. The combustion products of interest, CO₂, H₂O, NO₂ and NO were directed to the tube where NO₂ and NO gases were reduced to N₂ by copper at 650 °C. Thereafter the mixture of CO₂, H₂O and N₂ passed through three pairs of thermal conductivity cells and traps. H₂O was absorbed by Mg(ClO₄)₂, and after that CO₂ was absorbed by "Ascarite". The concentrations of CO₂, H₂O and N₂, which were related to the C, H and N contents in the sample, were determined based on the three thermal conductivities of the gas mixture. Sulfur was determined using the ASTM D-4294 method at CANMET. Oxygen was calculated by difference.

2.1.2 Heating Loss

This ASTM D-1509 method determines moisture present in the sample. About 2 g of the sample, weighed to the nearest 0.0001 g, was dried at 125 °C for 1 hr. After cooling in a desiccator the sample was reweighed and the weight loss reported as a weight percentage of the sample. Information on moisture content can also be obtained from Thermogravimetric Analysis (TGA). Results are the average of three determinations.

2.1.3 Ash

Ash in the char was determined by the ASTM D-1506 method. A 2 g sample, weighed to the nearest 0.0001 g, was placed in a constant weight crucible and heated for 16 hr in a muffle furnace at 550 °C. The ash residue was cooled in a desiccator and weighed. Results were expressed as a weight percentage of the sample and each are the average values of three determinations.

2.1.4 X-Ray Fluorescence (XRF)

About 0.5 g of the sample was ashed at 750 °C for 12 hr. The ash was then fused into a glass pellet at 1050 °C for 90 min. The glass pellet was analyzed by an XRF analyzer at CANMET. Results reveal the metal oxide content of the sample.

2.1.5 Thermogravimetric Analysis (TGA)

Organic fraction weight loss and ash content in the char were quantified by TGA at CANMET. Two types of experiments were conducted using a Perkin Elmer TGS-2 instrument. In the first, 10 mg of sample was heated under nitrogen flow from 30 °C to 950 °C with a heating rate of 10 °C/min then kept at 950 °C for 3 min. Three distinct weight losses were recorded and used to determine moisture (30 °C to 130 °C), volatiles (130 °C to 400 °C), and further weight loss (400 °C to 820 °C) assigned to decomposition of deposited hydrocarbons.

In the second experiment, 10 mg of sample was heated under a flow of N₂ with the heating rate of 10 °C/min from 30 °C to 830 °C, then kept at 830 °C for 30 min. At this point, the temperature was increased to 900 °C under a flow of N₂. When 900 °C was reached, the N₂ was replaced by an air flow for 20 min. The remaining sample was assigned as the ash content in the sample.

2.1.6 Atomic Absorption Spectroscopy (AAS)

A sample of 30 mg of ash was treated with 10 ml of a 5:1 concentrated HCl/HNO₃ mixture and heated on a hot plate until almost dry. Distilled water was added and the solution was filtered. Zinc, sodium, potassium, magnesium and calcium were determined on the

filtrate using flame AAS (Varian Techtron Model AA-5).

2.1.7 Iodine Number Surface Area

The ASTM D-1510 procedure was followed. An adequate preweighed amount of dry sample was placed into a glass test tube with stopper. The aqueous iodine solution (25.00 ml of 0.0473 N) was added and shaken for 1 min. The sample was filtered and the unadsorbed iodine in a 20.00 ml aliquot was titrated with 0.0394 N sodium thiosulfate using starch as an indicator.

2.1.8 Surface Area and Pore Size Distribution by Gas Adsorption

The gas adsorption measurements were completed with a Micromeritics ASAP 2010 gas adsorption porosimeter at Dalhousie University, Halifax. Approximately 1.0 g of sample was degassed at 250 °C under vacuum until no pressure change was observed. The sample was then transferred to the analysis system and degassed further at 250 °C with a turbo pump until the outgas rate in the manifold/sample holder couple was less than 60 mm Hg/min, similar to the outgas rate of the manifold alone. CO₂ or N₂ was then dosed onto the sample up to a relative pressure of 0.03 and 0.01 respectively (relative to the pressure in the sample holder), with equilibration indicated by a pressure change of 0.10 mm Hg/min or less. The operating temperature was -196 °C for N₂ and 0 °C for CO₂. The sample was then evacuated

to measure the desorption profile. Pore size analysis by the Density Functional Theory (DFT) Model was obtained using a slit shaped pore model to allow for a relative comparison between the samples. A least square fit model is used to correlate the model isotherms with the observed isotherm, which then gives a pore size distribution.

2.1.9 Toluene Discoloration

In order to provide information on the organic impurities present on char, the ASTM-D 1618 method was followed. About 2 g of the sample, weighed to the nearest 0.01 g, was mixed with 20.0 ± 0.2 ml of toluene and vigorously shaken for 1 min. Transmittance of the filtrate was measured at 425 nm using a Spectronic 20 D spectrophotometer. Toluene was used as a blank.

2.1.10 pH

The pH of the char and carbon black was measured using an Accumet pH Meter 910 (precision ± 0.05 pH) following the ASTM-D 1512 method. About 5 g of the sample, weighed to the nearest 0.01 g, was suspended in 50.0 ± 0.2 ml of CO₂ free distilled water and boiled for 15 min. After cooling to room temperature the pH was measured.

2.1.11 Particle Size Measurement

Particle size measurement was obtained by Transmission Electron Microscopy, (TEM). In spite of the difficulty in defining the boundaries of the particles this method remains the most accurate tool for particle size distribution [15]. The sample was embedded in epoxy resin and was left in an oven at 75 °C overnight to polymerize. A thin section was cut by a Reichert OMU 2 Ultramicrotome with a diamond knife and examined on a Zeiss-109 Electron Microscope at 80 kV with a magnification range from 30, 000 to 85, 000. The diameters of the particles were measured manually using enlarged micrographs. Particle size distribution curves were then plotted.

2.1.12 Aggregate Size Measurement

Aggregates of the char particles were measured by using a laser diffraction sizing technique (Malvern Particle Sizer 2600 Series), at Dalhousie University, Halifax. A monochromatic light beam from a low power helium-neon laser is diffracted from particle aggregates in an alcohol suspension containing 1 g of sample, weighed to the nearest 0.01 g. Scattered light is gathered by the detector when an electronic output signal which is proportional to the light energy, is measured at many separate angles of collection. The scattering angle of the light is related to the subject particle diameter. The measured diffraction pattern is analyzed by computer using non-linear least squares analysis to

calculate particle diameters and to plot their distribution.

2.1.13 Raman Spectroscopy

All Raman spectra were recorded using the Renishaw Ramanscope which features a CCD detector. The instrument was used in the point illumination mode. The wavelength of the Ar⁺ laser was 514 nm. The microscope was used to position the sample and focus the beam. Peak positions, their width and their areas were determined using a "Galatic" GRAMS 386 computer software.

2.1.14 Infrared Spectroscopy (FTIR)

Transmission Fourier-transform infrared spectroscopy data were collected from pressed KBr pellets using a Mattson-Polaris spectrometer in the region between 4000 cm⁻¹ and 700 cm⁻¹ and at a resolution of 2 cm⁻¹. Approximately 0.5 mg of a dry sample was ground with 300 mg of dry KBr. The pellet was then pressed under vacuum.

2.1.15 Scanning Electron Microscopy (SEM)

A Hitachi S570 Scanning Electron Microscope equipped with a backscattered electron detector and energy dispersive X-ray analyzer provided an overview of the elements

in an entire sample and at specific points using “SQ”-Standardless Quantitative Method, as well as information about the topography of the sample. A sample was embedded in epoxy resin, spread on the SEM stub to an approximately 1 mm thickness, and after drying, it was polished and carbon-coated. Alternatively, the sample was sprinkled on a double-sized sticky stub and coated with gold.

2.2 Char Demineralization

It was necessary to wet the “as-received” char with methanol before treatment. The 1:1:10 ratio (by weight) of the sample, methanol and acid (or base) was kept constant, while the acid (or base) concentration, the reaction time and temperature were variables in the experiments. After acid (or base) treatment the samples were filtered and rinsed with distilled water until the pH of the run-off was at or near neutral. The samples then were dried at 110 °C overnight.

2.3 Heat Treatment (Carbonization)

Approximately 30 g of char was loosely packed into a bed fixed by stainless steel and quartz wool plugs in a quartz tube (29 cm long and 3 cm in diameter). The tube was inserted into a Thermolyne Tube Furnace 2110 and purged with N₂ (250 ml/min) for 15 min prior to heating. The heating rate was 20 °C/min. The carbonization temperatures, 600, 700, 800 and

900 °C, were kept constant for 4 hr. The sample was cooled to room temperature under N₂ flow. A carbonization process was also carried out in the vertical furnace at CANMET Energy Technology Center (Ottawa). Description of the unit is given in Section 2.8. The carbonization conditions are given in Table 3.11.

2.4 Surface Group Analysis

Acidic surface groups such as carboxyl, lactone, phenol and carbonyl are quantified by Boehm titration [20]. Four bases, NaOC₂H₅, NaOH, Na₂CO₃ and NaHCO₃, with their widely different base strengths are theoretically able to neutralize these acid groups corresponding to their pK_a values. NaOC₂H₅, as the strongest base reacts with all groups; NaOH does not react with carbonyl groups; Na₂CO₃ does not react with carbonyl or phenolic groups; and NaHCO₃ reacts only with carboxyl groups. About 1 g of dry sample, weighed to the nearest 0.0001 g, was placed in each of four flasks and 50.00 ± 0.05 ml of 0.1000 N base was added to each. The mixtures were vigorously agitated for 48 hr on a mechanical shaker at room temperature. This length of time was shown by others [20] to be sufficient for establishing equilibrium. The chars were separated by filtration and aliquots of the filtrates were back-titrated with 0.1000 N HCl using methyl orange as an indicator. It is important to note that 0.1000 N NaOC₂H₅ was prepared in absolute (dry) alcohol and the 0.1000 N HCl titrant was in dry dioxane solution.

2.5 Oxygenated Surface Group Analysis by Pyrolysis GC-MS

Py-GC-MS experiments were carried out with a 120 Pyroprobe Pyrolyzer coupled to a Hewlett Packard HP 5890 Series II Gas Chromatograph equipped with an HP 5971A Mass Selective Detector. The pyrolysis parameters were: temperature 200 - 1000 °C in 100° steps, 20 seconds pyrolysis interval, ramp off and interface at 100 °C. GC parameters were: oven temperature 200 °C, split flow 20 ml/min and column pressure 15.0 psi; the GC column was a DB-5 (30 m x 0.25 mm id). A few milligrams of sample was placed in a quartz tube and sandwiched between quartz wool. Flash pyrolysis was performed in increments of 100 °C. Evolved CO and CO₂ (selected ions of 28 m/z and 44 m/z, respectively) were monitored by the mass spectrometer. These products originated from oxygenated acidic surface groups which were thermally decomposed upon pyrolysis [21].

2.6 Adsorption Capacity

2.6.1 Methylene Blue Adsorption

In this procedure 100.0 ml of aqueous 800.0 ppm methylene blue solution was added to about 0.5 g of the dry sample, weighed to the nearest 0.0001 g, and shaken at room temperature for 1 hr. After filtration, the concentration of unadsorbed methylene blue in solution was measured by optical absorption at 609 nm with a Spectronic 20 D spectrophotometer using a water blank.

2.6.2 Phenol Adsorption

About 0.5 g of dry sample, weighed to the nearest 0.0001 g, was mixed with 100.0 ml of aqueous 100.0 ppm phenol solution. The suspension was shaken on a mechanical shaker at room temperature for 24 hr. A decrease in phenol concentration, due to adsorption on char, was measured by the method of Bray and Thrope [22 and 23]. Briefly, to 1.0 ml of the sample placed into a 50 ml test tube, 1.0 ml of the 2 N Folin-Ciocalteu reagent and 2.0 ml of 20 % w/v sodium carbonate were added. The mixture was boiled in a water bath for 1 min then cooled in water to room temperature. The volume was made up to 25.0 ml and the absorbance read at 620 nm.

2.6.3 Metal Ions Adsorption

About 0.25 g of dry sample, weighed to the nearest 0.0001 g, was mixed with 100.0 ml solution containing about 100.0 ppm of the adsorbates Cu^{2+} or Pb^{2+} . The samples were left in contact on a mechanical shaker at room temperature for 24 hr. After that, the samples were filtered and the concentrations of the metal ions that remained in solution were determined by AAS [24].

2.7 Oxidation of Char

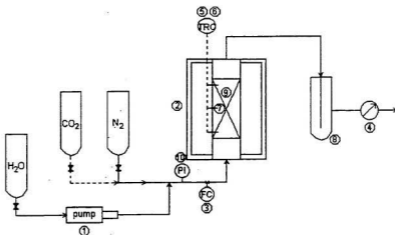
Air oxidation was carried out in the furnace used for carbonization (Section 2.3). After a carbonization step (600 °C, 4 hr) the sample was allowed to cool down. The temperature drop was stopped at 320 °C and N₂ was replaced by air with a flow rate of 250 ml/min, at 320 °C for 5 hr.

Hydrogen peroxide oxidation was carried out by placing the sample in contact with (aqueous) 10 % v/v H₂O₂ solution at room temperature, for 10 days. The char was filtered, washed thoroughly with water and dried at 110 °C overnight.

Another sample was oxidized using nitric acid by adding char to 50 % HNO₃ in the ratio 1:4 w/v in a beaker and stirred on a hot plate at 60° C for 5 hr. After cooling, the sample was filtered, rinsed with distilled water (to neutral pH) and dried at 110 °C overnight.

2.8 Char Activation

Char activation was carried out by physical activation in the Carbonization/Activation Unit shown schematically in Figure 2.1. The unit consists of a stainless steel tube which is inserted in the Lindberg vertical furnace. Three K-type thermocouples at different locations in the reactor tube were used to monitor temperature. An accurate flow meter (Siera) of 0 to



1. Harvard apparatus infusion/withdraw syringe pump
2. Vertical tube furnace
3. Mass flow controller
4. Wet test meter
5. Honeywell digital temperature controller
6. Digital temperature readout
7. Thermoelectric thermocouple
8. Cold finger trap
9. Reactor tube
10. Pressure gauge

Figure 2.1 Carbonization/Activation Unit

500 ml/min flow capacity was installed for gas flow control. The system included a syringe pump for periodic injection of water into a stream of N_2 gas when steam activation was performed.

The activation process consisted of two stages: Char carbonization, the first stage in the activation process, was performed to remove volatile materials and to pyrolyse remaining high molecular weight hydrocarbons. About 20 g of char was placed in the stainless steel tube, inserted into the furnace, heated under nitrogen flow (485 ml/min) at 20 °C/min to 900 °C and carbonized for 1 hr. Subsequently, in the second stage, the temperature of the unit was adjusted, under N_2 flow, to the desired activation temperature. N_2 was replaced by an activating agent such as CO_2 (pure stream) or steam (6 ml of H_2O /hr in N_2) or 2 % O_2 in a N_2 stream with the specified flow rate. The activation process was terminated after a specified reaction time. Table 3.18 lists activation conditions.

2.9 Use of Molasses as Binder

In each experiment, molasses (Crosby's Family Brand Cooking) was mixed with uncarbonized C1 char to form a paste. A small amount of water was added to allow better mixing. The paste was dried in an oven at 110 °C overnight and crushed into pieces – 5 mm diameter to prepare it for activation. The samples were activated with CO_2 (run XIV) and with steam (runs XV, XVI). Also, one sample with 20 % molasses was activated with steam

for only 1.5 hr (run XVII) to observe reaction time influences on activated char properties.

Activation runs XV, XVI and XVII were carried out without prior-carbonization.

CHAPTER 3

RESULTS

3.1 Bulk Analysis of Pyrolytic Char and Commercial Carbon Black

3.1.1 Samples

The commercial carbon black grades used as reference samples were provided by Columbian Chemicals (Hamilton, Ont.) and Cabot (Sarnia, Ont.).

Six samples of char produced by the CAR technology were provided by EnerVision Inc. (Halifax) and were designated as C1, C2, C3, C_{Y1}, C_{Y2} and C_F. C1, C2 and C3 were chars collected from 3 cyclones in series. The unit configuration was later changed and chars were collected from two cyclones (C_{Y1}, C_{Y2}) and an end filter (C_F). A seventh sample designated as C_M is a mixture of C1, C2 and C3 in the ratio 85:12:3. They were analyzed "as - received".

3.1.2 Physico-Chemical Properties

A wide range of carbon blacks were selected for comparison with the pyrolytic char. Their physico-chemical characteristics are given in Table 3.1 (iodine number, BET surface area, particle size, ash content, pH, toluene discoloration) and Table 3.2 (moisture, volatiles,

ash and elemental composition). Some of these values were provided by the supplier. Characteristic features of commercial carbon black are their low ash content and volatiles, high percentages of carbon, nm particle size and a wide range of surface areas (for different applications).

The physico-chemical characteristics of pyrolytic chars produced from CAR technology, pyrolytic chars from other studies and commercial carbon black are given in Table 3.2 (moisture, volatiles, ash and elemental composition). Table 3.3 compares iodine number, pH and toluene discoloration of pyrolytic chars only. In contrast to commercial carbon black, pyrolytic chars have higher ash content (8-18 %), higher percentage of hydrogen and sulfur and more condensed oil on the char (expressed as percentage of volatiles and toluene discoloration). Similar characteristics to carbon black are EnerVision char's iodine number and particle size (see Section 3.1.5 and 4.1).

For each kind of measurement made in this study, the random error introduced by the non-homogeneity of the samples exceeds the precision of the instrumentation by at least an order of magnitude. Some results include an extra digit beyond the last one strictly significant to avoid loss of information to anyone wishing to consult such data. (Standard deviations are also reported).

Table 3.1 Physico-Chemical Properties of Commercial Carbon Black Grades Used as Reference Standards

ASTM	Type	Iodine N ^o mg/g	Surf. Area BET, m ² /g	Average Part. Size, nm	Ash wt. %	pH	Toluene Discoloration % T	Applications [20]
N-115	SAF ¹	145	ND	ND	0.47	5.7	99.4	airplane, racing tire
N-234		141	116	26	0.68	ND	ND	
N-299		133	105	22	0.44	ND	ND	
N-330	HAF ²	89.2	80.0	30	0.12	7.5	71.8	sidewall, tire belt
N-550	FEF ³	47.7	42.0	56	0.23	7.5	86.2	extruded goods
N-660	GPF ⁴	42.3	30.0	55	0.28	7.9	64.2	tire carcasses, tubes

¹ SAF - super abrasion furnace black

² HAF - high abrasion furnace black

³ FEF - fast extruding furnace black

⁴ GPF - general purpose furnace black

ND - Not Determined

Table 3.2 Chemical Composition of Pyrolytic Char from Tire Pyrolysis by Different Investigators and of Commercial Carbon Black

Sample	Moisture to 125° C wt. % (±5 %)	Volatile to 400° C wt. % (± 10%)	Ash at 550° C wt. % (±10%)	wt. %					
				C	H	N	S	O	
C1	0.63	0.10	14.0	82.47	1.30	0.27	1.97	0.59	
C2	1.41	3.6	16.3	77.18	1.39	0.29	1.98	0.65	
C3	3.75	11.7	18.2	74.23	2.48	0.34	1.82	0.45	
C _M	0.82	1.65	14.4	81.59	1.35	0.27	1.97	0.58	
3	1*	0.20	2.80	11.4	85.17	0.74	0.76	ND	1.95
2*	0.50	2.00	8.6	ND	ND	ND	ND	ND	
3*	1.10	3.9	8.3	ND	ND	ND	ND	ND	
N-330	0.24	0.75	0.12	97.90	0.40	ND	0.60	0.70	
N-550	0.06	0.94	0.23	98.40	0.40	ND	0.60	0.40	
N-660	0.45	0.57	0.28	98.70	0.40	ND	0.50	0.20	

Triplicate analysis except for elemental analysis (single); ND - Not Determined

C1, C2, C3 and C_M are this study's samples as described in Section 3.1.1.

*1 Char recovered after vacuum pyrolysis at 500°C and 0.3 kPa, at Laval University by Rastegar, 1989 [25]

*2 Char recovered in pyrolysis processes by Kawakami, 1979 [6]

*3 Char recovered in pyrolysis processes by Takamura, 1982 [25]

Table 3.3 Physico-Chemical Characteristics of the Char Samples

Sample	Iodine N ^o , mg/g, (±15 %)	pH, (±7 %)	Toluene Discoloration, % T ₁ (±5 %)
C1	166	7.8	16.2
C2	135	7.3	1.2
C3	116	6.7	0.4
C _M	162	7.5	14.8
C _{V1}	137	ND	14.9
C _{V2}	123	ND	14.2
C _F	62.7	ND	5.4
1*	151.5	8.7	ND
2*	157.0	8.9	ND
3*	144.5	7.9	ND

C1, C2, C3, C_M, C_{V1}, C_{V2} and C_F are this studies samples as described in Section 3.1.1; ND-Not Determined

*1 Char recovered after vacuum pyrolysis at 500 °C and 0.3 kPa, by Rastegar, [25]

*2 Char recovered in pyrolysis processes by Kawakami, [6]

*3 Char recovered in pyrolysis processes by Takamura, [25]

3.1.3 Chemical Composition of Ash from Char

Three complementary methods were used to determine the ash composition of pyrolytic char. Table 3.4 lists the major elements (as % of ash) which can be determined by XRF. Si, Al, Ti, Zn, S and Ca constitute the major elements' oxides found in char derived from tires. Analysis of the ash by SEM-SQ Method (Table 3.5) show similar results for the major constituents. Finally, the alkali metals, Cu and Zn in ash were measured using AAS

(Table 3.6). All metals except Zn were below 1.1 % by weight (of ash). Zinc content ranged from 18.3 (filter char) to as high as 30.3 % (from 1st cyclone).

Table 3.4 Chemical Composition of Ash from Char by XRF Analysis

Oxide, wt. % ¹	C1	C2	C3
ZnO	35.9	25.6	22.3
SiO ₂	22.1	27.9	27.7
Al ₂ O ₃	11.5	16.3	18.5
TiO ₂	9.2	16.9	21.2
SO ₄ ²⁻	9.2	4.7	2.7
K ₂ O	0.8	0.6	0.5
Fe ₂ O ₃	2.3	1.7	1.6
P ₂ O ₅	0.7	0.4	0.6
CaO	5.3	3.5	2.7
MgO	1.5	1.2	1.1
Na ₂ O	1.5	1.2	1.1

¹ Single analysis; C1, C2 and C3 chars described in Section 3.1.1.

Table 3.5 Chemical Composition of Ash from Char by SEM-SQ Method

Oxide, wt. % ¹	C1	C2	C3	C _M	C _{Y1}	C _{Y2}	C _F
ZnO	20.5	11.7	20.7	19.4	16.0	16.4	12.3
SiO ₂	34.3	31.6	34.7	34.0	17.2	17.0	19.0
Al ₂ O ₃	16.4	20.5	15.9	16.9	6.7	9.9	12.8
TiO ₂	7.0	8.2	6.7	7.0	5.5	7.6	10.0
SO ₄ ²⁻	17.6	25.6	17.9	18.7	31.7	28.9	28.5
K ₂ O	0.7	0.3	0.9	0.7	0.2	0.2	0.4
Fe ₂ O ₃	ND	ND	ND	ND	0.4	0.5	0.4
CaO	2.6	1.8	2.5	2.5	0.6	1.0	0.1
MgO	ND	ND	ND	ND	0.6	1.4	1.3
Na ₂ O	ND	ND	ND	ND	20.2	15.7	15.2
CuO	0.9	0.3	0.7	0.8	0.9	1.4	ND

¹ Single analysis; Source of char samples described in Section 3.1.1; ND-Not Detected;

Table 3.6 Chemical Composition of Ash from Char by AAS

Element, wt.% ¹	C1	C2	C3	C _M	C _{Y1}	C _{Y2}	C _F
Zn	29.1	21.4	20.7	28.8	30.3	24.0	18.3
Na	1.03	1.00	0.81	0.75	0.90	0.55	0.70
K	0.70	0.66	0.56	0.56	0.51	0.45	0.37
Mg	0.45	0.43	0.44	0.44	0.51	0.55	0.41
Ca	0.30	0.14	0.15	0.24	0.26	0.12	0.06
Cu	0.15	0.07	0.07	0.11	0.04	0.08	0.15

¹Average of duplicate analysis, ±10 %; Source of char samples described in Section 3.1.1.

3.1.4 IR and Raman Spectroscopic Analysis

IR spectroscopic analysis was found to be unsuitable for the analysis of chars including activated and oxidized chars. The high adsorptive nature of carbon for IR radiation was the likely cause. Samples containing as low as 0.1 % char in KBr were still unsatisfactory for obtaining absorption bands for characteristic functional groups.

The structural order of char was studied by Raman spectroscopy. Figure 3.1 compares the Raman spectra of char as-received, carbonized char and carbon black while Table 3.7 lists important Raman spectral parameters such as G and D band frequencies, corresponding full width at half maxima and band intensity ratios. The G-band ($1580\text{-}1600\text{ cm}^{-1}$) and the D-band ($1350\text{-}1380\text{ cm}^{-1}$) frequencies and their widths are in correlation with crystallite forms in char. A shift in band intensity ratio after a carbonization process indicates major improvement in structural properties of the char comparable with those of commercial carbon black (N-330).

Table 3.7 Parameters of Raman Peaks of Char and Commercial Carbon Black

Sample	ν_G, cm^{-1}	ν_D, cm^{-1}	FWHM _G	FWHM _D	I_D/I_G
C1	1582	1357	106	243	1.85
C2	1586	1369	99	271	1.89
C3	1586	1370	96	266	1.82
Char carbonized at 900 °C	1583	1360	105	280	3.76
N-115	1584	1359	105	247	2.00
N-330	1586	1368	108	303	3.51

FWHM_G and FWHM_D, full width half maxima of the corresponding bands; I_D and I_G are intensities of D and G bands; C1, C2 and C3 are untreated char; Raman Spectra of C1, carbonized char and N-330 are shown in Figure 3.1

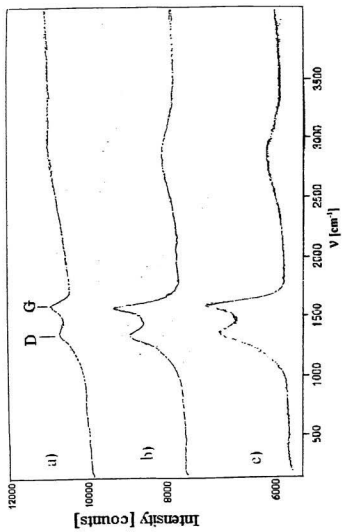


Figure 3.1 Raman Spectra of a) Untreated Char C1; b) Carbonized Char at 900 °C and c) Carbon Black (N-330)

3.1.5 SEM and TEM Micrographs

In this study transmission electron microscopy (TEM) was used to measure the particle size distribution in char aggregates. A thorough discussion of the TEM micrographs of untreated and carbonized char and commercial carbon black is presented in Chapter 4 (Figures 4.1 and 4.4).

Scanning electron microscopy (SEM) was used to compare the surface morphology of sample aggregates of carbonized and activated char. A thorough discussion of the scanning micrographs is presented in Chapter 4 (Figures 4.14 - 4.16).

3.1.6 Particle and Aggregate Size Distribution

Particle size distribution of untreated and carbonized char and carbon black were manually calculated from their magnified TEM micrographs (Figure 4.1 and 4.4). Their particle size distribution is discussed in Chapter 4 (Figure 4.2 and 4.5 a).

Aggregate size distribution was successfully measured with a laser diffraction sizing technique as described in Section 2.1.12. The aggregate size distributions of untreated and carbonized char and carbon black are discussed in Chapter 4 (Figures 4.3 and 4.5 b). The distributions follow a Gaussian curve with an average aggregate size of $\sim 19 \mu\text{m}$.

3.2 Demineralization of Char

An attempt was made to decrease the mineral impurities in char in order to improve its properties and market value.

Acid concentration, temperature and contact time are parameters which influenced the demineralization process. Ash content data as a function of H_2SO_4 concentration are given in Table 3.8. It can be seen that very little improvement was observed with H_2SO_4 concentrations above 0.5 M. The influence of reaction temperature on ash content (Table 3.8) showed 22-25 % increase in ash removal with higher temperature. Finally, the influence of contact time on ash content was measured. A treatment for 40 min was found sufficient. Almost 50 % of the ash can be removed by acid washing under suitable conditions.

AAS metal analysis (Table 3.9) of the resulting ash after demineralization show that Zn is the major ash constituent being removed. Concentrated acid washings can remove up to 99 % of Zn. More dilute acid solutions (i.e., 0.5 M H_2SO_4) are still able to remove as much as 80 % of initial Zn. The removal of other elements by acid washing was evaluated by SEM. As seen in Table 3.10 substantial amounts of Al, Ti and S could be removed.

Table 3.8 Ash Content of Char, wt. %, as a Function of Acid Concentration, Reaction Temperature and Time

H_2SO_4 , mol/L	0	0.05	0.25	0.5	1.0	3.0
60 °C, 40 min						
Ash ¹ of C _I	13.9	10.2	7.9	7.2	6.6	6.7
Ash ¹ of C _M	14.4	10.7	8.5	7.5	7.1	6.9
Reaction Temperature, °C	25		40		60	
1 M H ₂ SO ₄ , 40 min						
Ash ¹ of C _I	8.9		8.5		6.6	
Ash ¹ of C _M	9.1		8.8		7.1	
Reaction Time, min	10	20	30	40	50	60
1 M H ₂ SO ₄ , 60 °C						
Ash ¹ of C _I	9.4	9.1	8.8	6.6	6.7	6.6
Ash ¹ of C _M	9.7	9.4	9.1	7.1	6.9	6.9

C_I and C_M are untreated chars discussed in Section 3.1.1.

¹Average values of duplicate analysis, ± 10 %

Table 3.9 Zn Content in Ash of Chars Treated with Different Acids and Using Different Concentrations Measured by AAS

Acid concentration, mol/L	C ₁ , wt. % ¹	C _M , wt. % ¹
Before treatment	29.1	28.8
0.05 M H ₂ SO ₄	24.1	22.7
0.25 M H ₂ SO ₄	14.1	13.6
0.5 M H ₂ SO ₄	6.0	5.7
1 M H ₂ SO ₄	0.71	0.66
3 M H ₂ SO ₄	0.36	0.41
Conc. H ₂ SO ₄	0.32	0.36
Conc. HCl	0.15	0.71
Conc. HNO ₃	0.20	0.15
Conc. HCl/HNO ₃	0.26	0.22

¹ Average of duplicate analysis, ± 10 %; C₁ and C_M char samples described in Section 3.1.1.

Table 3.10 Acid Wash Efficiency of Other Elements Measured by SEM

Element, wt. % ¹	C ₁ + 1 M H ₂ SO ₄	C ₁ + HCl/HNO ₃
Al (initial 15.9)	11.7	9.4
Si (initial 29.1)	28.7	27.4
Ti (initial 10.8)	7.6	7.0
S (initial 15.7)	4.8	2.2

¹ Single Analysis

3.3 Carbonization of Char

Post-pyrolysis heat treatment (carbonization) experiments were conducted to free char from residue oil and consequently from characteristic odour as well. Char C1 was chosen as the test sample. The physico-chemical characteristics of carbonized char at various carbonization temperatures and using two different furnaces are listed in Table 3.11. The largest change as the result of carbonization is the removal of toluene-soluble hydrocarbons. The samples were found to be odourless even at 600 °C. Iodine number and ash decreased significantly at higher carbonization temperatures. Mass loss ranged from 1.33-7.10 % where highest burn-off was observed with the more efficient vertical furnace. Because of significant ash loss at high temperatures the ash was analyzed for metals which were expected to be most volatile. Table 3.12 lists the changes in Zn, Na, K and Mg content in char carbonization at various temperatures. All metals showed small losses during carbonization, some showing as much as 30 % removal at 900 °C carbonization.

Before adsorption capacities of the carbonized char were carried out, analysis of the acidic groups present on the surface was undertaken. As described in the experimental Section 2.4, this involves titration of various acidic groups with increasingly stronger bases. The results of acid group titration are given in Table 3.13. Negative results observed for carbonized chars indicate the presence of basic ash. A more thorough discussion of these results can be found in Section 4.3.2.

Table 3.11 Physico-Chemical Characteristics of Char C1 Carbonized at Different Temperatures

Temperature, °C	Ash, wt.%, ±10 %	BET, m ² /g	Iodine number, mg/g ±15 %	Toluene Discoloration, % T, ±5 %	Mass loss, wt. %, ±8 %
600	14.5	ND	128	99.5	1.33
600*	14.5	67	125	99.6	5.10
700	13.5	ND	128	99.8	1.37
800	12.7	ND	110	99.6	1.67
900*	12.5	91	102	99.6	7.10

*Carbonization was carried out at CANMET, N₂ flow 485 ml/min in the vertical furnace for 1hr
Triplicate analysis except for BET (single); ND-Not Determined

Table 3.12 Chemical Composition of Ash from Carbonized C1 by AAS

Temperature, °C	Zn, wt. % ±6 %	Na, wt. % ±10 %	K, wt. % ±8 %	Mg, wt. % ±12 %
C1 (untreated)	29.1	1.03	0.70	0.45
600	28.2	0.79	0.61	0.29
700	29.2	0.74	0.59	0.28
800	26.8	0.75	0.48	0.31
900	23.5	0.62	0.48	0.29

Duplicate analysis

Table 3.13 Titration of Acidic Groups of Carbonized Char and Commercial Carbon Black

Carbonization Temperature, °C	Base Titrant, meq/100g			
	NaHCO ₃	Na ₂ CO ₃	NaOH	NaOC ₂ H ₃
600	-0.50	1.14	6.99	-17.00
600*	2.39	6.64	12.14	-6.37
700	-1.43	1.88	7.03	-17.90
800	-1.16	-1.89	-2.38	-17.40
900*	2.20	1.88	13.25	8.65
N-115	2.40	3.90	20.10	29.99
N-660	3.25	4.50	14.10	15.28

Average of duplicate analysis, ± 10-15 %

* See footnote in Table 3.11

Studies were conducted to examine how effective carbonized chars were at removing metals and organics from aqueous solution and to compare the results with commercially available activated carbon samples, (Norit SA 3 and charcoal), which are known to be effective adsorbents. Table 3.14 lists the experimental results of adsorption capacities for methylene blue, phenol, Pb²⁺ and Cu²⁺. Poor results for phenol adsorption were observed, while the adsorption of the large molecular weight methylene blue was somewhat better. Excellent metal ion adsorption was noted, particularly for chars carbonized at lower temperatures.

Table 3.14 Adsorption Capacity of Carbonized Char and Commercial Active Carbon

Temperature, °C	Methylene blue, mg/g ± 9 %	Phenol, mg/g ± 16 %	Pb ²⁺ , mg/g ± 10 %	Cu ²⁺ , mg/g ± 10 %
600	49.7	0.90	26.2	17.7
600*	43.3	1.8	29.0	32.3
700	51.2	3.2	19.3	10.2
800	50.9	4.6	15.8	10.0
900*	51.7	9.8	18.5	10.4
Norit SA 3	143.5	38.1	41.0	22.8
Charcoal	152.4	32.1	20.7	5.1

*See footnote in Table 3.11; Triplicate analysis

3.4 Oxidation of Char

In order to enhance the adsorption capacity of the carbonized char its surface was modified by the generation of acidic surface groups using various oxidation processes. The char sample carbonized at 600 °C (4 hr) was chosen for this study. Mild oxidations were performed using air and hydrogen peroxide. More severe oxidation used hot HNO₃. Results of titration of acidic groups (Table 3.15) revealed a vast improvement in acid group content as compared to unoxidized char (Table 3.13), the more severe HNO₃ oxidation process showing the largest increase. Surprisingly, the surface area (measured as iodine number) of the H₂O₂ - and HNO₃ -oxidized char decreased by about 50 % (Table 3.16). The new adsorption capacities of the oxidized chars are listed in Table 3.16. Adsorption capacity for

organics and metals increased slightly for air-oxidized char but the H₂O₂-oxidized char showed a major decrease in metal adsorption capacity. Elemental analysis of the oxidized chars (Table 3.17) showed an expected increase in oxygen content as predicted from the acid group titration results (Table 3.15). It is also noteworthy that more than 50% of the sulfur content was removed by oxidation using H₂O₂ and HNO₃.

Table 3.15 Titration of Acidic Groups of Oxidized Char

Sample	Base Titrant, meq/100 g			
	NaHCO ₃	Na ₂ CO ₃	NaOH	NaOC ₂ H ₅
air oxidation	11.53	16.85	18.20	23.20
H ₂ O ₂ oxidation	11.15	18.10	27.30	37.00
HNO ₃ oxidation	17.96	20.62	38.18	49.89

Average of duplicate analysis, ±10-15 %

Table 3.16 Iodine Number of Oxidized Chars and Their Adsorption Capability for Methylene Blue, Phenol, Pb²⁺ and Cu²⁺

Sample	Iodine N ^o , mg/g ± 15 %	Methylene blue, mg/g ± 9 %	Phenol, mg/g ± 16 %	Pb ²⁺ , mg/g ± 10 %	Cu ²⁺ , mg/g ±10 %
air oxidation	102	54.0	2.60	31.6	24.5
H ₂ O ₂ oxidation	58.6	54.7	0.27	10.0	8.1
HNO ₃ oxidation	45.4	51.2	0.03	25.8	13.4

Triplicate analysis

Table 3.17 Elemental Analysis of Char Carbonized at 600 °C and Oxidized Char Samples

Sample	C, wt. %	H, wt. %	N, wt. %	S, wt. %	O, wt. %*
Carbonized at 600 °C	82.65	0.37	0.35	2.18	0.43
Oxidized by air	81.78	0.35	0.37	2.22	0.70
Oxidized by H ₂ O ₂	85.88	0.40	0.35	0.91	1.02
Oxidized by HNO ₃	87.53	0.42	0.58	0.80	3.23

*Measured by difference

3.5 Activated Char

The effects of oxidant, activation temperature and duration on mass loss and surface area of activated char products were studied and the results listed in Table 3.18. Since mass loss is an important economic and structural parameter in the activation process, measurement of the sample mass was recorded as soon as the sample was taken out of the furnace. For carbonized char (900 °C) C1 activation, mass losses ranged from 12 to 38 % and is a function of temperature and activation time. The highest surface area was observed in run IX when CO₂ was used at a temperature of 900 °C and for 420 min.

In order to study the influence of the pre-carbonization temperature on the extent of activation, run XIII was performed. Activated char previously carbonized at 600 °C gave similar results as those carbonized at 900 °C prior to activation (run III) and with lower mass

loss. Char which was previously acid-washed (run XII) showed slightly better surface area (compared to run XIII). Finally, a sample which was activated then air oxidized (run XVIII) was studied. Adsorption capacity experiments were performed on selected activated chars and the results are given in Table 3.19. For organic adsorption capacity, char activated by CO_2 showed superior performance and was comparable to commercial active carbon. Pb^{2+} ions adsorption remained the same as that for carbonized char (Table 3.14) while, surprisingly, Cu^{2+} ions adsorption capacity sharply decreased.

3.6 Use of Molasses as Binder

Addition of various amounts of molasses to char C1 (uncarbonized) was investigated as a means of improving the product's adsorption capacity as well as serving as a matrix to bind the fine char powder for pellet or granular activated char production. Results of mass loss and increase in surface area (activation runs XIV, XV, XVI and XVII) under various experimental conditions are listed in Table 3.18. Mass loss was substantial owing to the fact that molasses as organic matter was extensively burnt-off and because of the high water content (27.2 %) in the sample. The highest iodine number (331 mg/g) was obtained for steam activated 30 % molasses/char sample (run XVI). BET surface area for run XV (molasses 20 %) was measured at 422 m^2/g (Table 3.21).

Table 3.18 Char Activation Conditions

Run N ^o	Sample description	Method	°C	Flow rate, ml/min	Time, min	Mass loss ² , %	Iodine N ^o , mg/g
I	C1, carbonized at 900 °C	steam ¹	900	485	120	16.42	267
II	C1, carbonized at 900 °C	steam	900	485	60	13.43	ND
III	C1, carbonized at 900 °C	steam	900	485	180	25.87	277
IV	C1, carbonized at 900 °C	CO ₂	875	342	100	12.00	146
V	C1, carbonized at 900 °C	CO ₂	875	342	120	13.00	ND
VI	C1, carbonized at 900 °C	CO ₂	875	342	240	17.50	226
VII	C1, carbonized at 900 °C	CO ₂	875	342	420	27.00	283
VIII	C1, carbonized at 900 °C	CO ₂	875	342	420	25.50	283
IX	C1, carbonized at 900 °C	CO ₂	900	342	420	38.00	302
X	C1, carbonized at 900 °C	2 % O ₂	750	474	60	9.50	108
XI	C1, carbonized at 900 °C	2 % O ₂	725	474	240	15.40	113
XII	C1, carbonized at 900 °C & washed by H ₂ SO ₄	steam	900	485	180	19.80	297
XIII	C1, carbonized at 600 °C	steam	900	485	180	19.70	276
XIV	C1+15% molasses, carbonized at 900 °C	CO ₂	875	342	420	64.00	274
XV	uncarbonized C1+20% molasses;	steam	900	485	180	43.75	321
XVI	uncarbonized C1+30% molasses;	steam	900	485	180	51.10	331
XVII	uncarbonized C1+20% molasses;	steam	900	485	90	31.70	267
XVIII	C1, carbonized at 600 °C; activation + air oxidation	steam	900	485	180	19.70	286

¹Only 3 ml H₂O/hr injected in N₂ stream; ²Single analysis; ³Average of duplicate analysis ±15 %; Detailed description of methods are given in Experimental Section

It was observed that the content of acidic surface groups increased in the activated char when molasses as binder was used (Table 3.20). Molasses-blended activated char samples exhibited a significant increase in metal adsorption capacity (Table 3.21), particularly for Cu^{2+} , compared with activated char without molasses (Table 3.19). Adsorption capacities for organic adsorbates were comparable with activated chars.

Table 3.19 Surface Area and Adsorption Capacity of Activated Char and Commercial Active Carbon

Sample	Iodine N ^o mg/g $\pm 15\%$	BET, m ² /g	Methylene blue, mg/g $\pm 9\%$	Phenol, mg/g $\pm 16\%$	Pb ²⁺ , mg/g $\pm 10\%$	Cu ²⁺ , mg/g $\pm 10\%$
X (O ₂)	108	ND	66.8	4.4	21.7	6.9
XI (O ₂)	113	ND	67.0	7.0	24.7	6.4
III (steam)	277	ND	131.4	27.5	21.1	7.9
XII (steam)	276	272	126.5	26.2	17.7	3.9
XIII (steam)	274	303	125.5	27.4	21.6	4.3
XVIII (steam)	286	300	112.0	23.8	19.4	4.7
VIII (CO ₂)	283	269	152.7	30.4	18.7	4.6
IX (CO ₂)	302	ND	154.2	30.9	23.2	4.4
Charcoal	449	ND	152.4	32.1	20.7	5.1
Norit SA 3	671	667	143.4	38.1	50.0	23

Triplicate analysis except for BET (single analysis); ND-Not Determined

Table 3.20 Titration of Acidic Groups of Activated Char Blended with Molasses

Sample	Base Titrant, meq/100g			
	NaHCO ₃	Na ₂ CO ₃	NaOH	NaOC ₂ H ₅
XIV (char +15 % of molasses)	-8.30	-1.57	5.53	5.10
XV (char +20 % of molasses)	-2.50	2.71	2.48	21.34
XVI (char +30 % of molasses)	-5.50	-2.72	5.03	22.41

Average of duplicate analysis, ± 10-15 %

Table 3.21 Surface Area and Adsorption Capacity of Activated Char Blended with Molasses

Sample	Iodine N ^o , mg/g ±15 %	BET, m ² /g	Methylene blue, mg/g ±9 %	Phenol, mg/g ±16 %	Pb ²⁺ , mg/g ±10 %	Cu ²⁺ , mg/g ±10 %
XIV	297	ND	150.5	31.3	16.3	9.7
XV	321	422	128.6	28.8	25.1	6.3
XVI	331	ND	126.1	29.1	26.2	9.0

Triplicate analysis except BET (single analysis); Sample codes as in Table 3.20; ND-Not Determined

3. 7. Pore Size Distribution of Activated Char

Quality of the internal surface of the samples was determined by their pore size and distribution. In order to measure pore size distribution of activated chars, a Density Functional Theory Model, (DFT) [26] was used to calculate model isotherms and correlate them to experimental adsorption gas isotherms. DFT pore size distributions of char activated by CO₂ and steam derived from their adsorption isotherms are discussed in Chapter 4 (Figures 4.11 and 4.12).

CHAPTER 4

DISCUSSION

4.1 Physico-Chemical Properties of Untreated Pyrolytic Char

From Table 3.2, (chemical characteristics of char and commercial carbon black), it can be seen that there is high ash content in all char samples. This includes char derived from scrap tires analyzed by other investigators. High ash content is due to the presence of inorganic ingredients used in tire production. The volatile matter of char C1 was extremely low and, except for C3, all other pyrolytic char samples were comparable. Higher volatility in char C3 (11.7 %) indicates that the cyclone units were not kept hot further down the system and that increasing amounts of pyrolytic oil condensed on the char.

Elemental analysis of the untreated pyrolytic chars were compared with commercial carbon black (Table 3.2). Clearly, the carbon content in the char is lower due to its higher ash content. The ash content of chars is influenced by the kind of tire used and is usually independent of the pyrolysis technology. The elemental hydrogen content indicates the presence of residual hydrocarbons, and in carbon black it is low (0.40 %), its presence originating from hydrocarbon feedstock partially combusted in carbon black production. Pyrolytic char principally consists of the original carbon black plus char produced from

rubber pyrolysis along with condensed hydrocarbons. However, the amount of hydrocarbons (and therefore, hydrogen content) can be decreased by efficient char thermal treatment. The effectiveness of thermal treatment can be seen in the results of elemental analysis of char carbonized at 600 °C in Table 3.17 where the percentage of hydrogen is reduced to 0.37 %.

The elemental nitrogen content in the char studied here is slightly lower than that obtained from vacuum pyrolysis [25]. Nitrogen originates from additives used in tire production. Sulfur content ranges between 1.8 and 2.0 % and originates from sulfur used in the process of rubber vulcanization. Although not reported in Table 3.2, other pyrolysis technologies suggest similar sulfur contents [3]. This would indicate that sulfur content in char is also independent of the pyrolysis technology employed. The oxygen content in this study's char samples are in the same range as found in commercial carbon black.

The higher percentage of volatiles (125-400 °C) in C2 and C3, (Table 3.2) are in agreement with the results of toluene discoloration (Table 3.3). The results of toluene discoloration, a measurement of extractables as % transmittance, clearly indicates a significant amount of hydrocarbon by-products (oil) present in these samples. Their presence indicates the need for post-pyrolysis heat treatment (carbonization).

The iodine number is considered a principal parameter in char or carbon black characterization because of its direct relationship to their specific surface area. The iodine

numbers for all char samples are in agreement with those from pyrolytic char obtained by the other investigators (Table 3.3).

Inorganic matter referred to as “ash content” is of major concern in this study since it may be a limiting factor in higher value commercial applications of pyrolytic char. Hence, one objective in this study was to measure the amount of removable ash components by acid treatment and to determine which elements were removed (see Section 4.2). Although there are problems associated with non-homogeneity of samples, the results from XRF (Table 3.4), from SEM (Table 3.5) and AAS (Table 3.6) indicate the presence of significant amounts of inorganic matter, as would be expected from scrap tires.

Raman spectroscopy was used to determine the structural arrangement of carbon atoms in char as well as the degree of structural order. The Raman spectra of char are typical for carbonaceous materials or polycrystalline graphite as shown in Figure 3.1. The band at 2700 cm^{-1} is assigned to the C-H stretch. The G and D bands, characteristic of carbon structural order, are in the expected regions of $1580\text{-}1600\text{ cm}^{-1}$ and $1350\text{-}1380\text{ cm}^{-1}$, respectively. The G band corresponds to the E_{2g} vibrational mode (i.e., C-C aromatic layers). The D band results from breakdown of the symmetry of carbon atoms which are close to the edge of the graphitic sheet and tends to disappear during graphitization [27]. From Table 3.7, it can be seen that char samples and commercial carbon black exhibit similar G and D band frequencies and comparable FWHM_G and FWHM_D values. Untreated char showed I_D/I_G ratios

similar to carbon black N-115. However, carbonization increased the I_D/I_G ratios to values similar to N-330. The I_D/I_G ratio is a function of particle size and specific surface area as well as carbon structure. In general, the ratio increases with particle size decrease or with surface area increase [27].

The thickness of the sample analyzed by Raman spectroscopy is about 50 nm. Each sample was analyzed at ten different locations to obtain a representative result. Only one measurement revealed a crystallite of titanium dioxide. This result would indicate that most of the inorganic impurities present are occluded by carbon aggregates.

Particle size and aggregate size of char particles and their size distribution are very important for commercial applications. As can be seen in Figure 4.2, particle size distribution of char C1 is in the same size range as that of commercial carbon black N-299. Figure 4.3 shows aggregate size distribution of pyrolytic char as fit by a Gaussian curve. This is very promising for the CAR pyrolysis-technology as other authors [1] reported larger particle size for pyrolytic char produced by different technologies. The difference between particle sizes of char C1 and of pyrolytic char produced by vacuum pyrolysis [28] is of an order of magnitude. Analysis of the TEM micrographs (Figure 4.1) show that this study's char particles are uniformly spherical in shape and, along with their aggregates, have the same general appearance as those of commercial carbon black.

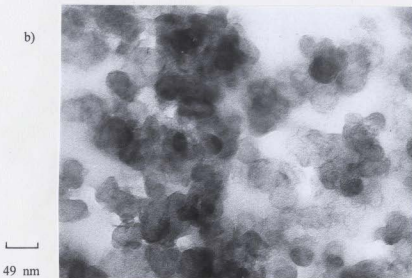
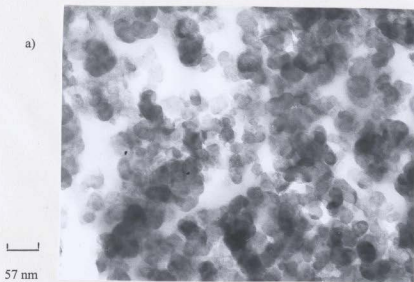


Figure 4.1 TEM Micrographs of (a) Char C1 and (b) Commercial Carbon Black

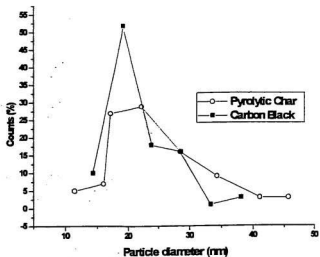


Figure 4.2 Particle Size Distribution Curves for Char C1 and Commercial Carbon Black (average of duplicate analysis)

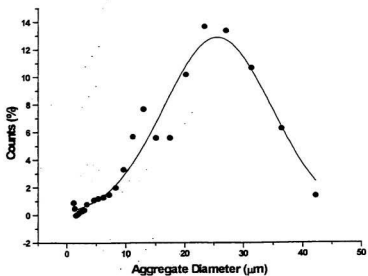


Figure 4.3 Aggregate Size Distribution of Char C1 (single analysis)

4.2 Char Demineralization

After reviewing the ash composition in char it was anticipated that most inorganics with the exception of Al_2O_3 , SiO_2 and TiO_2 , could be removed efficiently by acid treatment under suitable conditions. The key demineralization process parameters such as acid concentration, temperature and reaction time were varied while the char-to-acid solution ratio was kept constant. Demineralization using 1 M H_2SO_4 at 60 °C for 40 min was optimal (~50 % ash removal). Zinc was the major ash constituent to decrease under these conditions (98 % removal). Some of the Al, Ti and S oxides can be removed by 1 M H_2SO_4 , but better results were achieved by treatment with a concentrated acid mixture of HCl/ HNO_3 (Table 3.10).

Iodine number results of char C1 and C_M , washed by different acid concentrations, have a tendency to decrease with increase in acid concentration. This does not necessarily mean that the specific surface area of the char decreased. More likely, by-products formed during acid treatment adsorbed on the char surface, causing chemical interferences with iodine adsorption. Consequently, in such situations, the iodine number is not a reliable method for surface area determination and gas adsorption methods should be used.

4.3 Carbonization Process

4.3.1 Physical and Chemical Characteristics

The carbonization process was performed in both a horizontal furnace (at 600 °C, 700 °C and 800 °C) and in a vertical furnace (Carbonization/Activation Unit at CANMET at 600 °C and 900 °C). In all runs a small amount of yellowish-brown oil fraction with strong odour condensed out. This fraction represents most of the mass loss. Mass loss in the carbonization process using the horizontal furnace (4 hr) was much lower and in a narrow range (1.33-1.67 %). However, using the vertical furnace (only 1 hr) the registered mass loss ranged from 5.10 to 7.10 %. No char particle loss was observed. Therefore, differences in mass loss between the two furnace types may be explained by their different N₂ flow rates. The higher N₂ flow in the vertical furnace contributes to more efficient stripping out of volatilized hydrocarbons during the carbonization process. Furthermore, the higher mass loss at 900 °C may also be attributed to burn-off of carbon using the internal bound oxygen, from oxygenated functional groups, present in the char. All samples, including those carbonized at 600 °C, were totally freed of characteristic odour and their physico-chemical properties were observed to change. As shown in Table 3.11 toluene discoloration was almost nil and superior to that of furnace carbon black (Table 3.1). Ash content exhibits some decrease with increase in temperature. Ash differences of 2.0 % between samples carbonized at 600 °C and 900 °C may not be significant due to inhomogeneity of the samples, but this ash decrease at higher temperature is connected to certain metal mass loss as shown in Table 3.12. AAS analysis suggests that

the carbonization process decreases zinc content by 19 %, sodium by 40 %, potassium by 31 % and magnesium by 36 % relative to untreated char C1. If the decrease in these amounts are the result of evaporation, it would indicate that small amounts of these metals may be converted to organometallic species during the pyrolysis process.

Carbonized char exhibits the same wetting characteristics as commercial carbon black. This property is an advantageous for char applications. This is in contrast to uncarbonized char for which methanol was required to wet its surface before water suspension preparations.

Particle size, aggregate size and their distributions were not significantly changed by the carbonization process. This can be seen when comparing their TEM micrographs (Figure 4.4) with the corresponding micrographs of uncarbonized char (Figure 4.1) as well as their particle and aggregate size distribution (Figures 4.5 (a) and (b)), with Figures 4.2 and 4.3. Kawakami [6] suggested avoiding thermal treatment of char above 600 °C in order to preserve its reinforcing ability. However, the surface area of the carbonized char is not significantly changed at higher temperatures and, as observed by TEM, particle sizes and their aggregates show little change. Watson [29] suggested that reinforcement in terms of resistance to abrasive wear in tires is mainly influenced by the particle size of carbon black. The only way to check the char's reinforcing properties is by testing it in rubber industry laboratories. The char which was carbonized at 900 °C was examined in the rubber goods

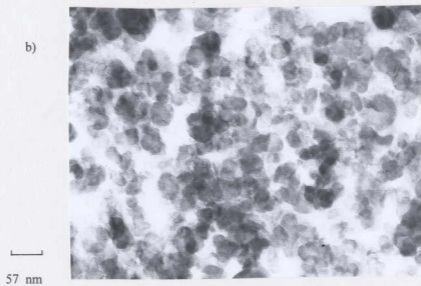
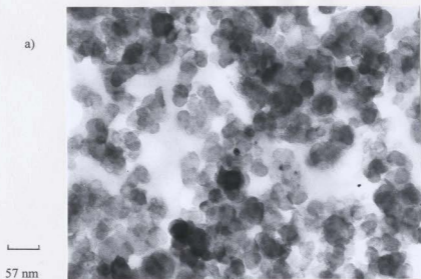


Figure 4.4 TEM Micrographs of Char Carbonized (a) at 600 °C and (b) at 900 °C

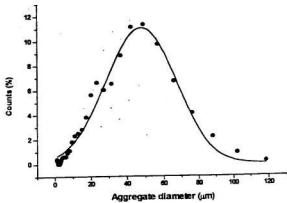
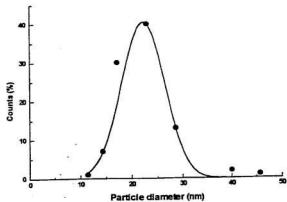


Figure 4.5 (a) Particle and (b) Aggregate Size Distribution of Carbonized Char at 900 °C (single analysis)

compounding facility “Hanna Rubber” (Ontario) in the applications which could tolerate higher ash content. The results obtained are very encouraging.

Iodine number values decreased with increase in carbonization temperature (Table 3.11). In this study the iodine numbers, a standard measurement of surface area, were confirmed to be in agreement with BET (surface area by gas adsorption) results in all samples except for untreated char (Figure 4.6). For example, the surface area for uncarbonized C1 determined by gas adsorption was $51 \text{ m}^2/\text{g}$ but that determined by iodine number was three times higher. In contrast, char C1 carbonized at $900 \text{ }^\circ\text{C}$ had BET surface area of $91 \text{ m}^2/\text{g}$ which was close to the surface area found by the iodine number of 102 mg/g . It was concluded that the iodine number determined for untreated char is more a measure of degree of impurity (hydrocarbons) than a measure of surface area. As discussed in Section 4.1, Raman spectra analysis showed carbon structure improvement with carbonization, and were comparable to those of commercial carbon black.

4.3.2 Adsorption Capacity

Since carbonized char has an appreciable surface area, its adsorption ability was investigated to examine its potential application as an inexpensive adsorbent for waste water treatment. The characterization of carbonized char was carried out in terms of its surface functional groups and its adsorptive capacity toward organic and metal adsorbates from

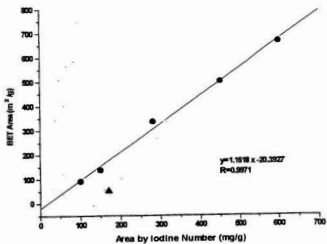


Figure 4.6 Correlation Between Surface Area Measured by BET and by Iodine Number
 Legend: ▲ Untreated Char
 ● Carbonized and Activated Chars

aqueous solutions.

All measurements of adsorption from aqueous solutions were obtained using a single point method, (instead of the adsorption isotherm method) [30], ensuring that the contact time employed was sufficient to reach steady-state conditions. The adsorption capacities of carbonized char for methylene blue, phenol, and metal ions Pb^{2+} and Cu^{2+} are listed in Table 3.14 and are compared to the adsorption capacity of active carbon references. Although the adsorption capacity of an adsorbent can be influenced by the pH of the solution [31], all adsorption experiments were done without adding buffer to control the pH. This was done to avoid interference of additional substances in the system since other studies of metal ions adsorption [32 and 33] indicate that buffer usage heavily influences metal ions adsorption on activated carbon. This is due to the fact that carbon itself is able to change the pH of slurries to pH values which are out of the range for optimum metal ions adsorption.

Very encouraging results for metal ions adsorption were obtained. Of the two carbonization units used, carbonized char obtained by the vertical furnace showed superior adsorption capacity for Pb^{2+} and Cu^{2+} ions. The metal ions adsorption capacity of char successively decreased as the carbonization temperature increased. As can be seen from Table 3.14 Pb^{2+} adsorption decreases by 29 % and Cu^{2+} by 41% over the 600-900 °C carbonization interval. Metal ions adsorption is assumed to be a function of acidic (negatively charged) groups present on the char surface [34]. Some of these groups may have

decomposed during carbonization at temperatures higher than 600 °C. However, there may be different processes involved in metal ions adsorption which cannot be fully explained here. It is recommended that char carbonized at 600 °C be looked at for future heavy metal ions adsorption applications.

In order to rationalize the differences in metal ions adsorption among the carbonized samples, the acidic groups were identified and quantified by the titration technique proposed by Boehm *et al.* [35, 36]. This technique is based on a sequence of neutralization reactions. Four basic titrants NaHCO_3 , Na_2CO_3 , NaOH and NaOC_2H_5 with different basicity are used in titrating carboxyl, lactone, phenol and carbonyl functional groups, respectively. In order to estimate the technique's validity two reference standards, carbon black N-115 and N-660, were analyzed and compared with the literature [37]. The carbon black results were in good agreement. The functional groups from titration results can be quantified (Table 3.13). Taking N-115 as an example; NaHCO_3 neutralization is related to the carboxyl group content and is found to be 2.40 meq/100 g; Na_2CO_3 is involved in both carboxyl and lactone neutralization, the lactone content therefore is the difference between 3.90 and 2.40, or 1.50 meq/100 g; NaOH titrates carboxyl, lactone and phenol, therefore the phenol content is the difference between 20.10 and 3.90, or 16.20 meq/100 g; finally NaOC_2H_5 , the strongest base, reacts with all four acidic groups present on the carbon surface, thus, carbonyl content is the difference between 29.99 and 20.10, or 9.89 meq/100 g. It is worth mentioning that the low ash content for carbon black N-115 (0.47 %) and N-660 (0.28 %) allows for acceptable

values. Actual values for acidic group contents will be lowered by the presence of basic groups on the sample surface. As well, lower or even negative results in Boehm titrations can be accounted for by high alkali ash content in samples. The HCl used in back-titrations would have to be used in neutralizing the alkali in the ash and any basic functional groups. The results for the carbonized char samples showed negative titration values due to high ash content. However, despite this difficulty, results showed an indication of the surface functionality which can be correlated with higher metal adsorption capacity.

4.4 Char Oxidation

Surface oxidation is a potential way to improve the adsorption efficiency of the char by increasing surface functional groups. Functional groups such as carboxyl, lactone, phenol and carbonyl are known to be widely involved in chemisorption processes [38].

Raman spectroscopy studies indicate that the untreated char possesses a low degree of carbon structural order. The oxidation rate on carbonaceous material is dependent upon the structural order (the lower the order, the higher the rate of oxidation). It was expected that mild oxidation by air or hydrogen peroxide, or an aggressive oxidation with diluted nitric acid would substantially modify the char surface by increasing the oxygen containing groups present. Functional group titration results (Table 3.15 and Figure 4.7) revealed a major surface group increase upon oxidation. Comparison of amounts of surface group generated

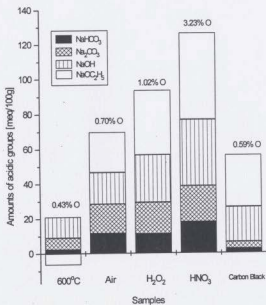


Figure 4.7 Classification of Surface Groups by Boehm Titration of Carbonized Char (600 °C), Oxidized by Air, by H₂O₂, by HNO₃ and Carbon Black N-115 (% oxygen present in samples also given above bars)

showed the following order: air at 320 °C < 10 % H₂O₂, 10 days < 50 % HNO₃ at 60 °C. This order was expected based on the strength of the oxidizing conditions. The actual values of surface group content are probably higher than those measured due to interferences in titration as discussed above. But support for the trend in these results can be found from oxygen content (Table 3.17). There was a reasonable correlation between oxygen content in the oxidized samples and amount of titratable acidic surface groups. Air oxidation increased the percentage of oxygen to 0.70 %, H₂O₂ to 1.02 %; and HNO₃, as the strongest oxidizing agent, elevated the oxygen content to 3.23 %.

Further information about oxygen-containing surface groups can be obtained from Temperature Programmed Desorption (TPD) profiles of CO and CO₂ by Py-GC-MS [21, 35, 39, 40]. Significant amounts of CO and CO₂ are evolved during pyrolysis (up to 1000 °C) of these oxidized chars. The CO and CO₂ products result from the thermal decomposition of acidic surface groups.

The appearance of CO₂ at a low pyrolysis temperatures is attributed to the decomposition of carboxylic groups which are the most sensitive to thermal decomposition. Lactone, phenol and carbonyl groups are more thermally stable groups and decompose at higher temperatures. According to a previous study [21] three distinct temperature ranges in the TPD profiles are of interest: 127 - 350 °C can be assigned to the decomposition of carboxylic acid groups to form CO₂; 350 - 550 °C assigned to the decomposition of lactone

groups evolving CO; and 550 - 1000 °C assigned to elimination of more stable phenol and carbonyl functional groups also in the form of CO. The ratio of CO and CO₂ measurement may not reveal good quantitative information about the presence of these groups because CO can also originate from the fragmentation (electron impact) of CO₂ in the mass spectrometer source. The TPD profiles of carbonized and air-oxidized char were compared (Figure 4.8) and the effects of surface chemistry modification by oxidation were confirmed by the increase in abundance (4 to 7 times) of CO and CO₂ generation.

In order to further support evidence of oxygen functionality on the char surface numerous FTIR spectra were recorded. However, FTIR appeared to be less informative in surface group determination than other methods. Char acts as a very effective black body absorber, markedly diminishing or completely attenuating beam energy throughput [21, 41, 42]. Even when the sample of the char was diluted enough by KBr to allow sufficient signal intensity through a transparent pellet, the concentration of acidic surface groups consequently fell below the limit of detection.

The adsorption capacity of oxidized chars were evaluated (Table 3.16). The iodine number of oxidized char decreases as the oxidizing agent strength increases. This may indicate that oxidized by-products were adsorbed on the carbon surface suppressing iodine adsorption. Air oxidation did not significantly affect the adsorption capacity of char for methylene blue but air oxidation improved adsorption of Pb²⁺ by up to 20 % and adsorption

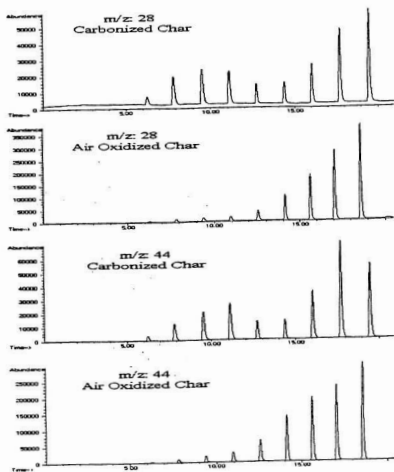


Figure 4.8 TPD Profiles of CO (m/z 28) and CO₂ (m/z 44) Production from Carbonized Char (600 °C) and Air Oxidized Char

of Cu^{2+} by 38 %. Chars oxidized by H_2O_2 and HNO_3 negatively affected the phenol adsorption. It is possible that oxidation by-products adsorbed on the char surface were able to repel phenol [40 and 43].

4. 5. Activation and Activated Char

Char derived from used tire pyrolysis is increasingly being studied as a raw material for the preparation of active carbon because of low cost and availability [1].

4.5.1 General Characteristics

In order to identify the appropriate experimental conditions for the most effective activated char production (for adsorption capacity) the most critical process parameters such as choice of oxidizing agent, activation temperature and residence time were studied (Table 3.18). Mass loss and iodine number were measured in activated chars and are viewed as important characteristics of the degree of activation.

Three series of the char C1 activations were performed using different oxidizing agents, different temperatures and different reaction times. The first series of activation were carried out using $\text{H}_2\text{O}/\text{N}_2$ stream (into N_2 flow of 485 ml/min, 6 ml of H_2O was injected in small increments per hr) at 900 °C for 1, 2 and 3 hr. The second series employed CO_2 with

a flow rate of 342 ml/min at 875 °C and 900 °C from 1.5 to 7 hr. In the third series 2 % O₂ in N₂ stream with a flow rate of 474 ml/min was used at temperatures of 725 °C and 750 °C for 1 and 4 hr.

In the third series, (activation by O₂), the low iodine numbers and high mass loss (Figure 4.9) indicate that the activation reactions, probably combustion of only disorganized carbon atoms were localized. The surface area of these samples remained at same level as for carbonized char and the adsorption capacity for test organic adsorbates did not significantly improve (Table 3.19). For these reasons, studies of activation by O₂ were limited.

In the first and second series, activated char was produced by steam and by CO₂ where results in mass loss ranged from 13.43-25.87 % and from 17.50-38.00 % respectively. As can be seen from Table 3.18 and Figure 4.9, weight loss (which is a function of the activation process temperature and residence time) can be roughly correlated to surface area (expressed by iodine numbers) of the activated char. As expected, the values of surface area increased with increasing treatment duration. Longer reaction time results in higher char burn-off, effecting the surface area of the char.

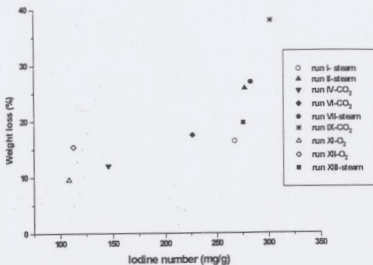


Figure 4.9 Correlation Between Surface Area and Mass Loss Resulting from Char Activation (Conditions of the activation runs are given in Table 3.18)

4.5.2 Porosity, Surface Area and Adsorption Capacity

Comparison of the changes on the char produced under different conditions can be based on parameters such as porosity, surface area and adsorption capacity. In general, the adsorptive capacities of solids are essentially related to the internal surface area, porosity and surface reactivity. These properties are linked to the texture of the surface, ash content and to the surface functional groups which are involved in both chemisorption and physisorption [32]. The specific surface area of the char samples activated by steam according to the iodine number range from 277 to 286 mg/g and according to N₂ adsorption measurements (BET) in the range 272 to 300 m²/g. The samples activated by CO₂ possess specific surface areas in the range 283 to 302 mg/g by iodine number, and 269 m²/g by BET N₂ adsorption. The results of surface area determined by iodine number and by N₂ adsorption for carbonized and activated char are in good agreement (Figure 4.6). Thus, iodine number can be a quick and inexpensive method for evaluation of char surface area [44]. By way of illustrating the differences in gas adsorption among samples, the adsorption/desorption isotherms of steam-activated chars are shown in Figure 4.10. The isotherm shapes with hysteresis loops are associated with mesoporous adsorbents where capillary condensation occurs [17]. It would indicate that steam creates mesopores in char during activation. The char/molasses mixture showed the best activation results.

The pore size and distribution of steam-activated chars, determined by a Density

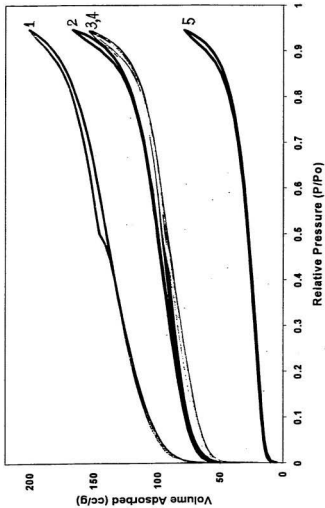


Figure 4.10 N₂ Adsorption/Desorption Isotherms of Steam Activated Chars
 Legend: 1) char blended with 20 % molasses; 2) steam activated and air oxidized; 3) steam activated and air oxidized, washed prior to activation; 4) acid washed prior to activation; 5) carbonized char at 600 °C

Functional Theory (DFT) Model, is shown in Figure 4.11. The results clearly indicate a significant widening of the pores originally present in carbonized char and the development of new pores with different width and volumes when steam is used. DFT pore size distribution analysis of CO₂-activated char shows that char reactivity is greater (higher pore volume) with CO₂ activation (Figure 4.12) than with steam (Figure 4.11). The literature [45] and our adsorption results (Table 3.19) suggest the opposite: that char reactivity at a given temperature is larger with steam than with CO₂. The larger molecules of CO₂ make diffusion through the pore system of the carbon particle more difficult and slower, with subsequent more limited accessibility to the micropores and a slower gasification rate. For example, active char (run III) produced by steam activation (3 hr at 900 °C) is comparable in adsorption properties (Table 3.19) with active char from run VIII produced by CO₂ activation (7 hr at 875 °C). In terms of yield, mass loss of the char in the steam activation process was the same as the mass loss in the activation by CO₂ (Table 3.18). Char activated by CO₂ at 900 °C for 7 hr (run IX) exhibits a larger surface area than that found in the sample from run VIII; their adsorption properties are the same if methylene blue and Pb²⁺ adsorptions are excluded, but mass loss is higher by 12.5 % at the higher temperature. Thus, it is clear that activation ended with large burn-off produced char with larger micropores, capable of higher adsorption toward methylene blue and Pb²⁺. Generally, the adsorption/desorption isotherms of CO₂-activated and carbonized char presented in Figure 4.13 are typical for microporous adsorbents [40 and 46].

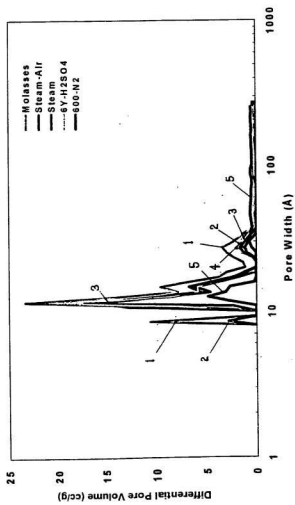


Figure 4.11 DFT Pore Size and Pore Volume Distribution of Steam Activated Char

Legend: 1) char blended with 20 % molasses; 2) steam activated and air oxidized; 3) steam activated; 4) acid washed prior to activation; 5) carbonized char at 600 °C

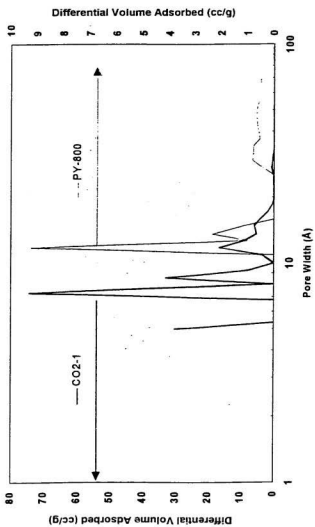


Figure 4.12 DFT Pore Size and Pore Volume Distribution of CO₂ Activated Char and its Precursor
 Legend: CO₂-1, CO₂ activated char; PY-800, carbonized char at 800 °C

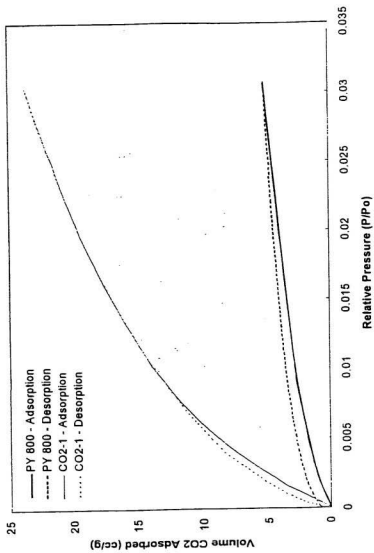


Figure 4.13 CO₂ Adsorption/Desorption Isotherms of Char Activated by CO₂
 Legend: PY-800, Carbonized Char at 800 °C; CO₂-1, CO₂-Activated Char

The surface topography, an important factor in adsorbent-adsorbate interactions, of the char was studied. SEM images of carbonized char at two different temperatures, shown in Figure 4.14, reveal dense and planar surfaces without notable cracks and crevices. It is clear that char obtained by pyrolysis has a disorganized structural pattern. As a result the level of surface energy (free energy) is low in exhibiting a desirable adsorption potential [47, 48 and 49]. Activation, considered as a modification of the geometrical and chemical structure of the char, contributes to its topographical change. As can be seen in Figure 4.15 the SEM micrographs of char activated by steam and CO₂ show pits and hollows as well as sharply defined steep cliffs denoted by curved lines. The adsorption capacity enhancement based on the adsorbent's topography [50] can be understood. Adsorption of methylene blue is not affected by the carbonization temperature (Table 3.14). However, the molecular dimensions of methylene blue, approximately 18 Å long and 9Å wide [51] allow for penetration into existing micropores of activated char samples. The DFT diagrams shown in Figure 4.11 and 4.12 indicate that activated char possesses larger number of micropores for access by such large molecules. In contrast, the pore volume and pore distribution of carbonized char is very limited.

Results from Table 3.16 indicate that the acidic groups produced by char oxidation with different oxidizing agents fail to attract positively charged methylene blue ions from aqueous solution. In some cases unidentified substituent groups on the carbon surface hinder dye adsorption [51]. Thus the expected results of higher adsorption capacity were not obtained. The same results are seen for steam-activated and air oxidized char (run XVIII

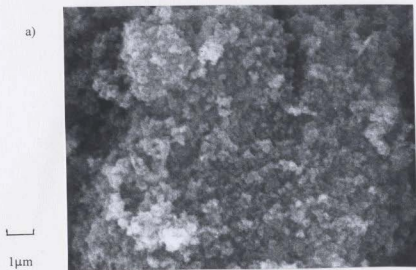


Figure 4.14 SEM Micrographs of Char Carbonized (a) at 600 °C and (b) at 900 °C

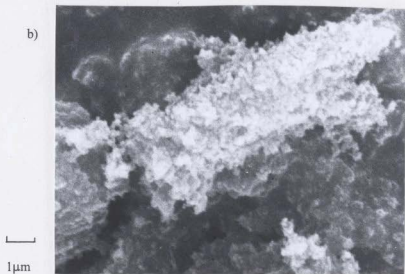


Figure 4.15 SEM Micrographs of Char Activated (a) by Steam and (b) by CO_2

compared with run XIII (Table 3.19)).

Amounts of methylene blue adsorbed increased considerably with char activation because of both the widening and the increase in degree of microporosity. As can be seen in Table 3.19, both samples of char activated by CO₂ are superior to reference standards.

Phenol adsorption capacity increases with increase in char carbonization temperature but is well below the capacity of activated char and commercial active carbons (Table 3.14). Phenol adsorption of the CO₂-activated char is comparable with that of commercial active carbons (Table 3.19). These results suggest that some pores in carbonized char are not accessible to phenol molecules and accessibility increases only upon activation as the result of pore enlargement. The extent of phenol adsorption has been found to be affected by the area of the surface and its chemistry [52].

Activation of char did not improve metal ions adsorption (Table 3.19) compared to carbonized char (Table 3.14). This observation would indicate that certain metal ions up-take is not related to improved surface area.

4.6 Molasses as Binder

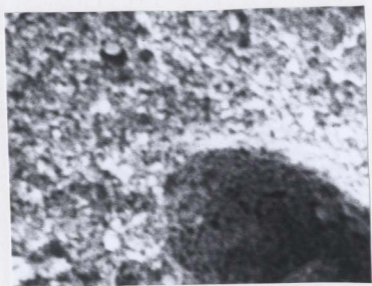
The fine powdery nature of activated char can limit its use in adsorption applications.

In order to produce extrudates for a granular activated char production, molasses as a binder was used. Molasses and lignosulphonate binders are commonly used in carbon black pelletization [15 and 37]. Although the hardness of the samples was not measured, it was observed that molasses imparted strength to the char material and appears to be a very good choice as a binder in pyrolytic char pelletization. The mass loss in the activation of the sample with added molasses was high (runs XIV-XVI), but it was compensated for by the increase of surface area, topography change (Figure 4.16) and higher adsorption capacity (Table 3.21).

4.7 Other Activation Studies

Steam activation followed by air oxidation (run XCVIII) did not show improvement in adsorption capacity [53, 54, 55]. Despite the fact that the surface area is slightly larger (Table 3.19) and Boehm titration shows a significant increase of acidic surface groups (much higher in comparison to steam activated, non-oxidized char, run XIII), adsorption capacity was not improved.

In order to study the influence of carbonization temperature prior to the activation process a sample was carbonized at 600 °C instead of at 900 °C, i.e., run XIII. Results of the activated char's adsorption capacity (Table 3.19) indicate that there was no significant qualitative difference between this activated char and run XIII whose precursor was pre-



1 μm

Figure 4.16 SEM Micrographs of Char Blended with 20 % Molasses Followed by Activation Using Steam

carbonized at 900 °C. As well, activation runs XV and XVI were performed without prior carbonization and the adsorption capacities obtained (Table 3.21) were satisfactory. These results indicate that a carbonization stage does not significantly influence the structural properties of the activated char. Therefore a prior carbonization of char in activation processes may be avoided, thus lowering the cost.

Untreated char, a normal precursor for carbonized or activated char production, contains 14.0 % ash with Zn as a major-acid removable fraction. Most minerals tend to remain in the char structure after carbonization or activation. This may limit their adsorbent applications. The ash possesses a very low surface area of 8.6 m²/g [3]. Due to the existing relationship between surface area and carbon content in the parent material, it was expected that a higher surface area would be obtained and consequently better adsorption ability of the char would be generated if acid-washed char was used for activation. In one experiment carbonized char was washed with 1 M H₂SO₄ removing ~ 50 % of the ash. The acid-washed char was then activated (run XII) by steam under the same conditions as an unwashed char (run III). The surface areas of pre-acid washed and activated char and of the unwashed, activated (Table 3.19 and Figure 4.10 and 4.11) were similar and so were their adsorption capacities. Thus the lowering of ash in chars before activation is not important.

It is noteworthy that in usage of carbonized char and activated char for waste water treatment, high ash content may not be a serious drawback. Most common precursors of

active carbons such as lignite and bituminous coal [34] have ash content often exceeding 20 % [32]. But tests must be performed to observe whether harmful metals are leached out of the chars when used in water treatment purifications.

CHAPTER 5

SUMMARY

This study on char samples produced by pyrolysis using the CAR process showed that this technology is capable of producing char with comparable morphological properties, (i.e., particle and aggregate size) to those of carbon black initially used in tire production. This makes the CAR technology unique to other presently available pyrolysis technologies. The other physico-chemical properties of the char are comparable to those of chars obtained by other investigators using vacuum, rotary kiln and fluidized bed pyrolysis reactor technologies. However, comparison of pyrolytic char with the commercial carbon black grades indicates the need for additional treatments to improve its properties.

The high ash content in char produced from scrap tire pyrolysis is a major difference when compared with commercial carbon black and thereby limits its use for tire manufacturing. Inorganic components in ash originate not only from compounds used in the original tire production but also from road use, e.g., sand. Therefore, a surface-washing treatment of the tire before pyrolysis could benefit char quality. This study showed no evidence of significant Fe present in the ash, indicating very efficient steel belt removal during tire particle production. Optimized demineralization conditions (1M H₂SO₄ at 60 °C for 40 min) proved to be an efficient way to decrease ash content in half in one step. Zn, a

major acid-removable constituent, was decreased by up to 98%. Al, Ti and S content were also significantly decreased. It may be advisable to focus future work at optimizing a hydrogenation process to remove Si as SiH_4 .

Post-pyrolysis heat treatment (carbonization) is an efficient method for residual hydrocarbon and odour elimination. Carbonization at low temperatures, i.e., 600 °C, contributes to an odourless char with hydrophilic character, improved structural order and low toluene discoloration values. Char's main morphological properties such as particle and aggregate size, surface area and dispersibility were preserved and consequently its reinforcing potential comparable to commercial carbon black. Carbonized char may meet some of the requirements for rubber compounding in certain applications where high ash content could be tolerated.

Carbonization of char at 600 °C is an excellent and cheap way of producing an inexpensive and effective adsorbent for waste water treatment. Carbonized char with its limited microporous nature exhibits some adsorption capacity for organic adsorbates such as methylene blue or phenol, but well below that of commercial active carbon. However, carbonized char has excellent adsorption potential for heavy metal ions, better than any studies using activated char or commercial charcoal.

The ability of char to chemisorb oxygen was very high. Oxidation treatments of

carbonized and activated char samples caused distinctive changes in the surface acidity. Both mild and more severe oxidation processes resulted in an increase in carboxyl, lactone, phenol and carbonyl surface groups. However, the contribution of these groups to increased aqueous adsorption capacity of studied adsorbates seems to be negligible. It has been suggested that carbonized pyrolytic char is a good adsorbent for SO₂, mercury, NO_x, dioxan, furans etc [13]. Therefore, acidic group participation in these gas adsorption applications may be fruitful in future studies.

This study showed that it is feasible to convert char derived from scrap tire into activated char using steam or CO₂ with acceptable yields. The activated char exhibits high aqueous adsorption affinity for high molecular weight organic species and reasonable adsorption for heavy metal ions. Activation experiments demonstrated that the activated chars of similar surface areas and porosities (consequently similar adsorption abilities) were produced either by 342 ml/min of pure CO₂ and with 6 ml/hr of H₂O in a N₂ stream (485 ml/min). It may be beneficial to increase H₂O injection in a N₂ stream in order to produce an even better activated char. A carbonization process prior to activation does not seem to benefit in improvement of activated char, therefore carbonization before the activation process may be avoided.

Partial ash removal prior to activation did not contribute in an expected increase in surface area and porosity development. Demineralization may be needed in some activated

char applications (i.e., drinking water purification, chemical clean-up application).

Molasses as a binder is a good choice to impart strength and increase adsorption capacity of activated char. A very good granulated active char can be produced. Further work should be directed at optimizing the use of other binders such as lignosulphonate and other natural waste materials.

REFERENCES

- (1) San Miguel Q., Fowler D. G. and Sollars C.J., (1998). "Pyrolysis of Tire Rubber: Porosity and Adsorption Characteristics of the Pyrolytic Chars", Ind. Eng. Chem. Res. 37, 2430-2435.
- (2) Williams P.T., Besler S. and Taylor T.D., (1990). "The Pyrolysis of Scrap Automotive Tires", Fuel, 69, 1474-1482.
- (3) Teng H., Serio M. A., Bassilakis R., Morrison P. W. and Solomon P.R., (1992). "Reprocessing of Used Tires into Activated Carbon and other Products", Am. Chem. Soc., Div. of Fuel Chem., 37, 533-547.
- (4) Merchant A. A. and Petrich M. A., (1993). "Pyrolysis of Scrap Tires and Conversion of Chars to Activated Carbon", AIChE Journal, 39, 1370-1376.
- (5) Beckman J.A., Crane G., Elefritz R.A., Kay E.L., and Laman J.R., (1977). "Reclamation of Scrap Tires" National Tire Disposal Symposium, Washington, DC. 14-15 June.
- (6) Kawakami S., Inoue K., Tanaka H. and Sakai T., (1980). "Pyrolysis Process for Scrap Tires", Am. Chem. Soc. Symposium Series 130, Washington DC., 557-571.
- (7) Crane G., Elefritz R., Kay E.L., and Laman J.R., (1978). "Scrap Tire Disposal Procedure", Rubber Chem. Technol., 51, 577-599
- (8) Dodds, J., Domenico W.F., Evans D.R., Fish L.W., Lassaher P.L., and Toth W.J.,

- (1983). "Scrap Tires: A Resource and technology Evaluation of Tire Pyrolysis and Other Selected Alternate Technologies", N.T.I.S. Report EGG-1241, 11.
- (9) Roy C., Rastegar A., Kaligauine S. and Darmstadt H., (1995). "Physicochemical Properties of Carbon Blacks from Vacuum Pyrolysis of Used Tires", Plastics, Rubber Composites Proc. Appl., 23, 21-30.
- (10) Luchessi A. and Maschio Q., (1983). "Semi-Active Carbon and Aromatics Produced by Pyrolysis of Scrap Tires", Conservation and Recycling, 6, 85-90.
- (11) Torkai N., Meguro T., and Nakamura Y., (1979). "Pyrolysis of Scrap Tires", Nippon Kagaku Kaishi, 11, 1604-1612.
- (12) Ogasawara S., Kuroda M., and Wakao N., (1987). "Preparation of Activated Carbon by Thermal Decomposition of Used Automotive Tires", Ind. Eng. Chem. Res. 26, 2552-2556.
- (13) Lehmann C. M.B., Rastam-Abadi M., Road M. and Sun J., (1998). "Reprocessing and Reuse of Waste Tire Rubber to Solve Air-Quality Related Problems", Energy and Fuels, 12, 1095-1099.
- (14) Black J. W., and Brown D.B., (1991). "Castle Capital Inc. CAR Technology" Newsletter.
- (15) Donnet J.B., Bansal R.C. and Wang M. J., "Carbon Black", 2nd Edition, Marcel Dekker Inc., New York (1993).
- (16) Wang M. J. and Wolf S., (1991). "Filler-Elastomer Instructions Part III. Carbon-Black-Surface Energies and Interactions with Elastomer Analogs", Rubber Chem.

Technol., **64**, 714-736.

- (17) Patrick J. W., "Porosity in Carbons", Halsted Press, John Wiley & Sons, Inc. New York, Toronto (1995).
- (18) Smisek M. and Cerny S., "Active Carbon Manufacture, Properties and Applications", Elsevier Publishing Co., New York (1970).
- (19) Mattson J. S. and Mark B. H., "Activated Carbon Surface Chemistry and Adsorption from Solution", Marcel Dekker Inc., New York (1971).
- (20) Polania A., Papirer E., Donnet J.B. and Dagois G., (1993). "Modification et Interaction des Fonctions Oxygénées en Surface des Charbons Actifs", Carbon, **31**, 473-479.
- (21) De la Puente G., Pis J. J., Menendez J.A. and Grauge P., (1997). "Thermal Stability of Oxygenated Functions in Activated Carbons", J. Anal. Appl. Pyrolysis, **43**, 125-138.
- (22) Bevia F.R., Rico D. P. and Gomis A. F. M., (1984). "Activated Carbon from Almond Shells. Chemical Activation. I. Activating Reagent Selection and Variables Influence", Ind. Eng. Prod. Res. Dev. **23**, 266-271.
- (23) Glick David, "Methods of Biochemical Analysis", Interscience Publishers, Inc., John Wiley & Sons, New York, 45-53 (1954).
- (24) Budinova T.K., Gergova K. M., Petrov N. V. and Monkova V. N., (1994). "Removal of Metal Ions from Aqueous Solution by Activated Carbons Obtained from Different Raw Materials", J. Chem. Tech. Biotechnol., **60**, 177-182.

- (25) Rastegar A., "Characterization of the Carbon Black Produced by Vacuum Pyrolysis of Scrap Rubber and Optimization of the Pyrolysis Parameters", Master Thesis, University of Laval, Quebec, (1989).
- (26) Oliver J. P. and Conklin W. B., (1996). "Determination of Pore Size Distribution from Density Functional Theoretic Models of Adsorption and Condensation within Porous Solids", Micrometrics Instrument Corporation, Inc. Norcross, GA 30093 USA, Appendix A-2 - A-27.
- (27) Darmstadt H., Lümmchen L., Roland U., Roy C., Kaliaguine S. and Adnot A., (1997). "Surface vs. Bulk Chemistry of Pyrolytic Carbon Blacks by SIMS and Raman Spectroscopy", Surf. Interference Anal., **25**, 245-253.
- (28) Shaola A., Darmstadt H. and Roy C., (1996). "Acid-Base Method for The Demineralization of Pyrolytic Carbon Black", Fuel Processing Technol., **46**, 1-15.
- (29) Watson W. F., (1955). "Combination of Rubber and Carbon Black on Cold Mining", Ind. Eng. Chem., **46**, 1281-1290.
- (30) Linares-Solano A., Rodríguez-Reinoso F., Molina-Sabio M. and Lopez-Gonzales J. D., (1984). "The Two-Stage Air-CO₂ Activation in The Preparation of Activated Carbons. II. Characterization by Adsorption from Solution", Ads. Sci. Techn., **1**, 223-234.
- (31) Moreno-Castilla C., Rivera-Utrila J., Lopez-Ramon M. V. and Carasco-Marin F., (1995). "Adsorption of Some Substituted Phenols on Activated Carbons from a Bituminous Coal", Carbon, **33**, 845-851.

- (32) Finueneisel G., Zimny T., Albinak A., Siemieniowska T., Vogt D. and Weberl J. V., (1998). "Cheap Adsorbent. Part 1: Active Cokes from Lignites and Improvement of Their Adsorptive Properties by Mild Oxidation", Fuel, 27, 549-556.
- (33) Toles C.A., Marshall W. E. and Johns M.M., (1997). "Granular Activated Carbons from Nutshells for The Uptake of Metals and Organic Compounds", Carbon 35, 1407-1414.
- (34) Toles C.A., Marshall W. E. and Jones M.M., (1997). "Mining the Potential of Pecans", Water Technol., 2, 92-98.
- (35) Donnet J.B., (1968). "The Chemical Reactivity of Carbons", Carbon, 6, 161-176.
- (36) Oda H. and Yokokawa C. (1983). "Effect of Surface Acidity of Activated Carbons on Their Characteristics of Adsorption from the Vapor Phase Comparison of Retention Time for Carbons Used as Adsorbents for Gas Chromatography", Carbon 21, 303-309.
- (37) Donnet J. B. and Voet A., "Carbon Black, Physics, Chemistry and Elastomers Reinforcements", Marcel Dekker Inc., New York, (1976).
- (38) Oda H., Kishida M. and Yokokawa C. (1981). "Adsorption of Benzoic Acid and Phenol from Aqueous Solution by Activated Carbons. Effect of Surface Acidity", Carbon, 19, 243-248.
- (39) Muniz J., Herrero E. J. and Fertes B. A., (1998). "Treatments to Enhance the SO₂ Capture by Activated Carbon Fibers", Appl. Catal. B: Environ. 18, 171-179.
- (40) Papirer E., Li S. and Donnet J. B., (1987). "Contribution to The Study of Basic

- Groups on Carbons", Carbon, 25, 243-247.
- (41) Gomez-Serrano V., Pastor-Villegas J., Prez-Florindo A., Duranait-Valle C. and Valenzuela-Calahorro C., (1996). "FT-IR Study of Rockrose and of Char and Activated Carbon", J. Anal. Appl. Pyrolysis, 36, 71-80.
- (42) Starsinic M., Taylor R. L., Walker P. L. and Painter P. C., (1983). "FTIR Studies of Saran Chars", Carbon, 21, 69-74.
- (43) Deng X., Yinghong Y. and Gao Z., (1997). "Preparation and Characterization of Active Carbon Adsorbents for Wastewater Treatment from Eluthrilithe", J. Colloid Interface Sci., 192, 475-480.
- (44) Molina-Sabio M., Salina-Martinez de Lecea C. and Rodriguez-Reinoso F., (1985). "A Comparison of Different Tests to Evaluate The Apparent Surface Area of Activated Carbons", Carbon, 23, 91-96.
- (45) Rodriguez-Reinoso F., Molina-Sabio M. and Gonzales M. T., (1995). "The Use of Steam and CO₂ as Activating Agents in The Preparation of Activated Carbons", Carbon, 33, 15-23.
- (46) Dubinin M. M., (1982). "Microporous Structures of Carbonaceous Adsorbents", Carbon, 20, 195-200.
- (47) Everett D. H., (1993). "Some Problems in The Study of the Heterogeneity of Solid Surfaces", Amer. Chem. Soc., Langmuir 9, 2586-2592.
- (48) Lebod R., (1994). "The Porous Structure of Active Carbons Modified with Glucose Pyrolysis Products", Mater. Chem. Phys., 36, 256-263.

- (49) Markovic V., (1987). "Use of Coal for Pitch in Carbon/Carbon Composites", Fuel, 66, 1512-1515.
- (50) Huhl H., Kashani Motlagh M. M., Muhlen H. J. and Van Heek K. H., (1992). "Controlled Gasification of Different Carbon Materials and Development of Pore Structure", Fuel, 71, 879-882.
- (51) Graham D., (1955). "Characterization of Physical Adsorption Systems. III. The Separate Effects of Pore Size and Surface Acidity upon The Adsorbent Capacities of Activated Carbons", J. Phys. Chem., 59, 896-900.
- (52) Mahajan O. P., Moreno-Castlla C. and Walker P. L., (1980). "Surface-Treated Activated Carbon for Removal of Phenol from Water", Sep. Sci. Technol., 15, 1733-1752.
- (53) Rodriguez-Reinoso F., Linars-Solano A. and Martin-Martinez J. M., (1984). "The Controlled Reaction of Active Carbons with Air at 350° C-II", Carbon, 22, 123-130.
- (54) Pis J. J., Mahamud M., Pajaris J. A., Parra J. B. and Bansal R. C. (1998). "Preparation of Active Carbons from Coal", Fuel Process. Technol., 57, 149-161.
- (55) Mikhalowsky S. V., Glushakov V.G. and Noscov A. M., (1994). "Influence of Porous Structure of Active Carbons on The Chemical Transformation of Surface Functional Groups", Stud. Surf. Sci. Catal., 87, 705-713.



